Review

Current Trends in the Utilization of Photolysis and Photocatalysis Treatment Processes for the Remediation of Dye Wastewater: A Short Review

S M Anisuzzaman [1], Collin G. Joseph [2,3,4,*], Chuan Kian Pang [2,4], Nur Ammarah Affandi [2,4], Sitti Nurazida Maruja [2,4] and Veena Vijayan [2,4]

[1] Chemical Engineering Programme, Faculty of Engineering, Universiti Malaysia Sabah, Kota Kinabalu 88400, Sabah, Malaysia; anis_zaman@ums.edu.my
[2] Sonophotochemistry Research Group, Faculty of Science and Natural Resources, Universiti Malaysia Sabah, Kota Kinabalu 88400, Sabah, Malaysia; kian8808@gmail.com (C.K.P.); ms1821030t@student.ums.edu.my (N.A.A.); bs18110574@student.ums.edu.my (S.N.M.); veenavijayan@ums.edu.my (V.V.)
[3] Water Research Unit, Faculty of Science and Natural Resources, Universiti Malaysia Sabah, Kota Kinabalu 88400, Sabah, Malaysia
[4] Industrial Chemistry Programme, Faculty of Science and Natural Resources, Universiti Malaysia Sabah, Kota Kinabalu 88400, Sabah, Malaysia
[*] Correspondence: collin@ums.edu.my; Tel.: +60-88-320000 (ext. 2117)

Abstract: Development in the textile industry leads to an increased demand for the use of various dyes. Moreover, there is the use of some dyes in the food industry as well as medical diagnostics. Thereby, increased demand for dyes in various fields has resulted in dye-containing wastewater. Only a small portion of the generated wastewater is adequately treated. The rest is usually dumped or otherwise directly discharged into the sewage system, which ultimately enters rivers, lakes, and streams. The handling and disposal of such concentrated wastewater, especially the dye-containing wastewater, is considered to be a major environmental issue from the moment of its generation to its ultimate disposal. Conventional water treatment methods such as flotation, filtration, adsorption, etc., are non-destructive physical separation processes. They only transfer the pollutants to other phases, thereby generating concentrated deposits. The advanced oxidation process (AOP) is one of the most effective emerging methods for the treatment of wastewater containing chemical pollutants. The method involves the formation and interaction of highly reactive hydroxyl radicals under suitable activation conditions. These radicals are non-selective and efficient for the destruction and eventual mineralization of recalcitrant organic pollutants. This review aims at the pros and cons of using photocatalysis as an efficient AOP to degrade dye-containing wastewater.

Keywords: photolysis; photocatalysis; photodegradation; degradation efficiency; UV irradiation

1. Introduction

Dyes can be described as the substances used to impart color to a given substrate in various industries such as silk, paper, and paints [1]. Dyes can be classified in multiple ways based on industrial applications and by their chemical types or chromophore structures [2]. Dyes are characterized by the capacity to absorb light radiation in the visible spectrum, which is the wavelength from 380 to 750 nm [1]. Dyes are organic compounds consisting of two groups in their molecules, which are the chromophore and the auxochrome [3]. The most common chromophores of dyes are azo ($-N=N-$), nitro ($-NO_2$), nitroso ($-N=O$), thiocarbonyl ($-C=S$), and alkenes ($-C=C-$) [3]. The chromophore is the active site of the dyes, which is the absorbing part of the visible spectrum. The electronic properties of the chromophore result in the color imparted by the dyes [1]. The auxochrome in the

chromogenic molecules may intensify the color of the dye and acidic groups such as SO_3 and COOH are frequently introduced into dye structures to enhance their solubility [4].

Table 1 shows the classification of dyes based on their applications. Dyes also can be divided into cationic, anionic, and non-ionic dyes. Cationic dyes have cationic functional groups that may dissolve into positively charged ions in an aqueous solution, such as Methylene blue (MB), Rhodamine B (RhB), Malachite green (MG), Rhodamine 6G (Rh6G), and Crystal violet (CV). Because the onium group is the most frequent cationic functional group, most of the cations are N^+ ions. Anionic dyes include Acid orange 7 (AO7), Eosin Y (EY), Methyl orange (MO), Acid red 14 (AR14), Alizarin red S (ARS), Rose Bengal (RB), Phenol red (PR), etc. Anionic functional groups are found in all anionic dyes [5].

Table 1. Classification of dyes based on industrial application.

Industrial Application Class	Applications	Chemical Type/Chromophore Structure	Example
Disperse dye (non-ionic)	Polyester, nylon, cellulose, cellulose acetate, acrylic fibers, polyamide, plastics	Azo, nitro, styryl, anthraquinone, benzodifuranone,	Disperse violet 26 (DV26), Disperse blue 27 (DB27)
Direct dye (anionic)	Paper, cellulose fibers, nylon, rayon, cotton, viscose, leather	Azo, oxazine, thiazole, stibene, phthalocyanine	Direct red 28 (DR28), Direct orange 26 (DR26)
Reactive dye (anionic)	Cellulose fibers, silk, cotton, wool fibers, nylon	Anthraquinone, formazan, oxazine, phthalocyanine, azo, triphenylmethane	Reactive blue 19 (RB19), Reactive blue 5 (RB5)
Vat dye (non-ionic)	Cellulose fibers, cotton, viscose, wool	Anthraquinone, Indigoid	Vat blue 1 (VB1), Vat blue 4 (VB4)
Basic dye (cationic)	Acrylic, ink, paper, silk, wool, cotton, treated nylon, modified polyester, polyacrylonitrile	Triarylmethane, azo, xanthene, Triphenylmethane, hemicyanine, cyanine, acridine, diazahemicyanine, anthraquinone, oxazine, thiazine	Basic blue 6 (BB6), MB, MG
Acid dye (anionic)	Nylon, wool, leather, food, silk, cotton, cosmetics, ink-jet printing, paper, modified acrylics	Anthraquinone, xanthene, azo, nitrodiphenylamine, triphenylmethane, nitroso, azine, nitro, indigoid	AO7, Acid yellow 36 (AY36)

Source: Morsy et al. [2]; Hunger [6]; Katheresan et al. [7].

Ensuring the availability of clean water is essential for humans and terrestrial and aquatic animals and plants. In compliance with the sustainable development goals (SDG) to ensure this availability in the pursuit of global economic growth and industrial developments, generated wastewater has to be treated and remediated for reuse. Textile industries comprise one of the most labor-intensive industries, providing employment to various downstream and upstream sectors. At the same time, this industry produces a large amount of dye-contaminated wastewater that is released into rivers and streams. Modern dyes are synthetically designed to withstand weathering processes or biodegradation. Over the last few decades, researchers and scientists have investigated new techniques and methods to treat and remediate dye-contaminated wastewater. This review paper explores the current and updated trends in this field with a focus on photolysis and photocatalysis treatment processes.

Occurrence of Dyes in the Aquatic Environment

In the last few decades, the contamination of water by dyes has continuously existed due to the release of dyes from industrial textile discharge. In Malaysia, the textile and dyestuff industry is one of the developing industries that contribute to the country's economic growth. However, these dyestuff industries require high water consumption, which produces a massive quantity of pollutants and is often disposed into water bodies with

little to no pre-treatment, leading to critical environmental problems [8]. The wastewater discharged from the dyestuff industries has been considered the primary source of water contamination and pollution [9]. Owing to the presence of aromatic rings and reactive ring groups such as sulfur and naphthol along with heavy metals such as chromium, lead, copper, cadmium, and mercury, textile wastewater is regarded as highly toxic [4].

The basic textile processing technology includes desizing, scouring, bleaching, mercerizing, and the dyeing process. The different dyes, inorganic and organic-based compounds used in the wet processing, etc., will influence the wastewater components [10]. Wet processes often use many chemicals and large quantities of water; 1 kg (kg) of fabric requires around 80–150 m^3 of water [11]. Table 2 shows the wet processes producing textile wastewater in which the dyeing, printing, and finishing steps give the most contribution to fluctuations in water quality parameters such as pH, temperature, COD, BOD, color, and salinity.

Table 2. Textile wastewater produced by wet processes.

Process	Quality of Textile Effluent
Desizing	High TSS, high BOD, neutral pH
Scouring	High TTS, high BOD, high alkalinity, high temperature
Bleaching, Mercerizing	High TSS, high BOD, alkaline wastewater
Heat-setting	Low TSS, low BOD, alkaline wastewater
Dyeing, printing, and finishing	High TSS, BOD, COD, wasted dyes, neutral to alkaline wastewater

Source: Naveed and Bhatti, [12].

2. Dye-Removal Methods

Dyes are noticeable even in small amounts and present as more aesthetically displeasing in contaminated wastewater bodies [6]. Moreover, many dyes are hazardous for aquatic organisms and humans. Hence, the interest in the treatment of dye wastewater for reuse has been great due to the shortage of clean, natural water sources [2]. An effective method is a must to remove large amounts of dyes rapidly, cost-effectively, and without producing secondary contaminants [7]. Conventional dye removal methods have been classified into three main categories, which are physical, chemical, and biological methods.

2.1. Physical

Physical methods are primarily used to separate large dissolved matter and to recover and reuse valuable substances used in the main processes [13]. Many physical technologies have been applied to the removal of dyes, such as ion exchange, adsorption, and the membrane filtration method [14]. The coagulation or flocculation process is primarily utilized for the effective removal of dispersed dyes. However, it has the downside of increasing sludge formation volume [2,15]. This treatment method is commonly applied as a pre-treatment step for the removal of dyes from effluents [16]. Filtration methods such as reverse osmosis, microfiltration, and nanofiltration are used to remove the dyes from water for reuse, but this technique is not cost-effective, as it requires high maintenance costs [2]. Another physical method is the adsorption, which is more efficient for the decolorization of dyes than the coagulation method. It uses low-cost adsorbents such as polymeric resins and bentonite clay, but it is not cost-efficient as the adsorbents are usually used once without being able to reuse [2].

2.2. Biological

Biological treatment is a widely used technique in wastewater treatment that has been used for over 150 years [6]. This technique is based on the activated sludge that contains a variety of aerobic and anaerobic microorganisms such as bacteria and green algae [4]. The biological method is preferred over physical and chemical practices as no

hazardous by-products are produced, and it is a more cost-effective method on an industrial scale [2]. Laccase is one of the examples of enzymes of interest for dye removal due to its physicochemical properties as a promising biocatalyst. The mechanism of laccase on dye degradation is by catalyzing three types of reaction: the direct oxidation of phenolic substances, the indirect oxidation of non-phenolic substrates, and coupling reactions with reactive intermediate radicals formed during direct oxidation [2]. However, despite the advantages of the biological method, its effectiveness for dye removal is limited since many dyes are not biodegradable and are toxic to microbes as synthetic dyes are designed in such a manner.

2.3. Chemical

The chemical method of dye removal can be classified into two categories, which are conventional chemical treatments and chemical oxidation processes [17]. In conventional chemical treatment methods, treatments such as adsorption using various adsorbents, coagulation, and flocculation methods and electrochemical methods merely transform the organic pollutants from one phase to another, i.e., causing secondary pollution [6]. The advantages of the conventional chemical method are lower sludge generation and high pollutant removal efficiency, while high operational and chemical costs and secondary waste are some of the disadvantages of chemical treatment methods [4]. Among the chemical methods, oxidation is effective and practical for large-scale wastewater treatment [18]. Chemical oxidation degrades organic molecules by using powerful oxidizing chemicals such as ozone, hydrogen peroxide, chlorine, and potassium permanganate [6]. The fundamental chemical oxidation process happens naturally when air and oxygen are present, but it is insufficient for heavily contaminated wastewater. Hence, there is a significant necessity to develop methods that can remove the pollutants effectively.

3. Advanced Oxidation Processes (AOPs)

In recent years, advanced oxidation processes (AOPs), which use combinations of ultraviolet irradiation, catalysts, and oxidants to produce hydroxyl radicals ($^\bullet$OH) in solutions have received attention as a technology for the degradation of harmful organic compounds in wastewater. AOPs were first proposed for the treatment of drinking water in the 1980s and later AOPs have been utilized for the treatment of various types of wastewaters [19]. Due to the complicated aromatic structure and resistant nature of dyes and compounds, conventional biological and chemical oxidation approaches are ineffective for the degradation of these compounds [20]. AOPs are viewed as a highly competitive technology in water treatment for removing organic pollutants that are not biodegradable and inactivating pathogenic microorganisms that cannot be treated with traditional techniques [21]. AOPs are mainly used to destroy organic contaminants in water and sewage [19].

In order to identify the formation as well as the reaction mechanism of reactive oxygen species (ROS) in each of the AOP systems, it is critical to study the principles and the degradation mechanism of organic pollutants under these AOPs. The presence of ROS is termed as responsible for the effective mineralization of various organic pollutants under different AOPs. ROS can be produced by external energy sources such as photo, sono, electro, etc., in the presence and absence of catalysts as well as secondary oxidants. AOPs are the oxidation processes that require the rapid generation of hydroxyl radicals ($^\bullet$OH), which is a highly reactive oxygen species, in sufficient quantities to allow the organic contaminants to be oxidized and mineralized by the free radicals to mineral salts, water, and carbon dioxide [22]. Hydroxyl radicals are non-selective in nature and can react with a wide variety of pollutants without any other additives, with rate constants typically in the order of 10^6 to 10^9 mol. l.s.$^{-1}$ [13]. AOPs start with the generation of OH radicals which then attack the targeted pollutants [22]. After the process of AOP methods, new oxidized intermediates are produced with lower molecular weights, or in the case of complete mineralization, carbon dioxide and water are produced [13].

AOPs can be classified based on homogenous and heterogenous reactions and based on the presence of irradiation (Figure 1). Homogenous reactions occur in a single phase. Meanwhile, a heterogenous reaction is when the reactants are components of two or more phases, in which, in AOPs, the pollutant is liquid and the catalyst is solid [23–25]. There are many developed methods of AOPs for wastewater treatment processes, as the basic chemical oxidation process is not enough for severely contaminated wastewater [18]. The literature has shown that hydroxyl radicals with high oxidizing potential can be generated through different types of AOPs for the degradation of dyes such as photocatalysis [26], photolysis, UV/H_2O_2 [27], photolysis, UV/O_3 [28], photo-Fenton [29], electrochemical oxidation [30], ozonation [31], and sonolysis [32]. The benefits of AOPs include rapid reaction rates and non-selective oxidation, which allows multiple pollutants to be treated at the same time and can reduce the toxicity of the pollutants. Mineralization can be completed by AOPs, but it can be costly, thus biological treatment is preferable for the final stage of the treatment of dyes [33].
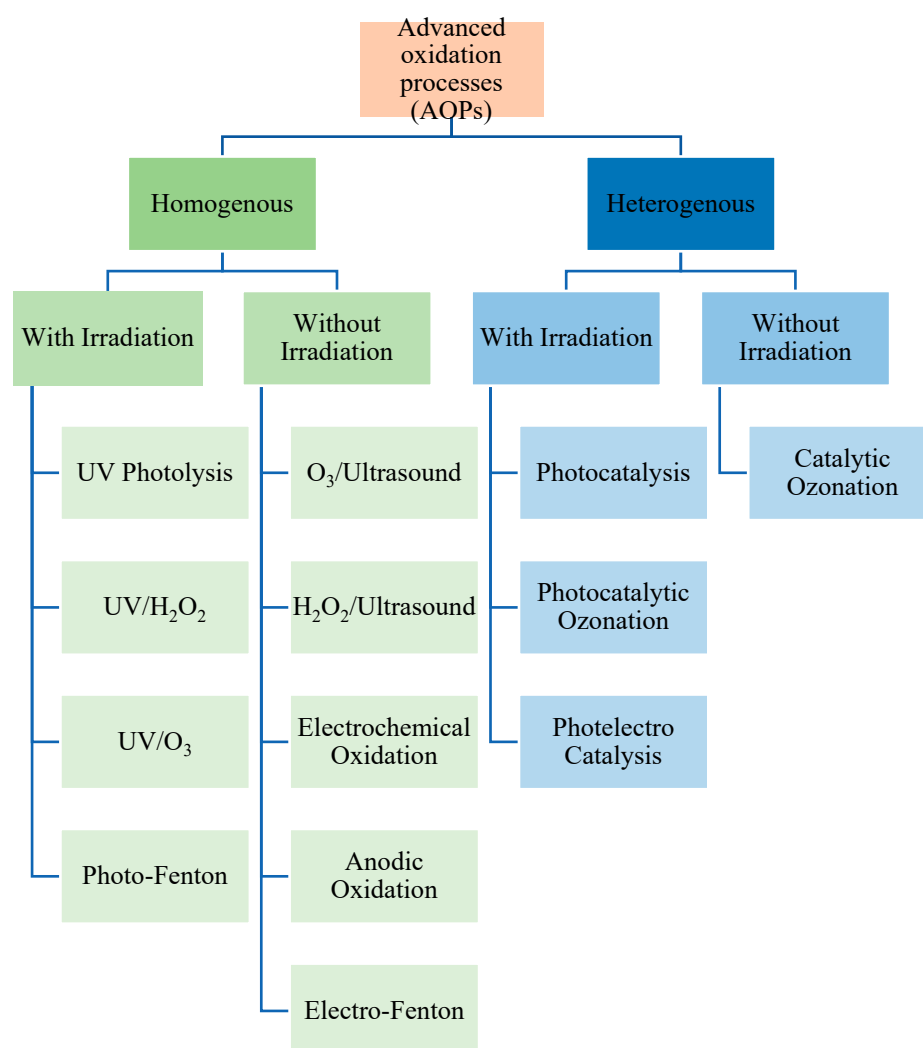

Figure 1. Different AOP-based treatment methods. Source: Khan et al. [34].

4. Photochemical Treatment of Dyes

Photodegradation is one example of an advanced oxidation process (AOP). This method is the chemical breakdown of a large molecule into non-toxic molecules in which the process of hydroxyl radicals initiated by photons absorbed in the wavelength of UV, visible, and infra-red (IR) spectral ranges, with or without the presence of a catalyst or oxidants [19,34]. Hydroxyl radical generation can be accelerated by the combinations of some commonly

used oxidants. The photodegradation of dyes is considered the most promising technology for the treatment of industrial wastewater processes as it is environmentally friendly, low-cost, and does not cause any secondary pollution [35]. The techniques available for the photodegradation of dyes are UV photolysis, photooxidation by oxidizing agents including hydroxyl radicals, hydrogen peroxide, ozone, and photocatalytic UV oxidation [34].

History

Humans first used photochemistry in 1500, when Canaanite peoples arrived along the Mediterranean's eastern shore. The current organic photochemistry stage began in 1866 when Russian scientist Carl Julius von Fritzche found that when a concentrated anthracene solution was subjected to UV light, it precipitated. This precipitation occurs as a result of anthracene molecules joining together in pairs, or dimers, which are no longer soluble. Scientists have found that the materials (dyes and phosphors) must have the capability to absorb optical radiation. Photocatalysis studies using TiO_2 have been reported since the early 20th century. In 1938, the photodegradation of dyes by TiO_2 was reported. UV absorption produces active oxygen species on the TiO_2 surface, causing the photodegradation of dyes. It was also discovered that TiO_2 did not alter throughout the photoreaction, despite the fact that the photocatalyst terminology was not used for TiO_2 in the paper and it was instead referred to as a photosensitizer [36].

5. Current Developments in UV Radiation Sources

Ultraviolet (UV) radiation is in the electromagnetic spectrum that human eyes cannot see [23–25]. There are three classifications of UV radiation based on the interaction of UV radiation with biological materials, which are UV-A (400–315 nm), UV-B (315–280 nm), and UV-C (280–100 nm) [23–25]. UV-A, also known as black light, is related to skin aging and has recently been linked to skin cancer in humans and animals. UV-B is also associated with the risk of skin cancer and it contributes to erythema (sunburn), but in contrast, it is also important in the synthesis of vitamin D, which suggests that it may potentially reduce the risk of prostate, breast, and colon cancer and is also used in phototherapy for baby jaundice [37]. UV-C's effects on organisms are negligible, as it is completely filtered out by the Earth's atmosphere, but UV-C is valuable as a research tool and a sterilizing procedure due to its bactericidal properties at wavelengths of 260–280 nm [25,37]. UV light is used in these photochemical techniques due to the greater energy of their photons, as shown by Planck's equation [38]:

$$E_\lambda = hc/\lambda \tag{1}$$

where E_λ is the energy of a photon, λ is the wavelength of the radiation, h is the Planck's constant, and c is the speed of light.

Different types of sources have been used in photochemical AOPs for dye degradation, such as high-pressure mercury lamps (infrared radiation, UV, and visible range), low-pressure mercury lamps (λ_{max} = 254 nm), pulsed UV lamps, ultraviolet light-emitting diodes (UV LEDs), microwave-powered electrodeless discharge lamps (λ_{max} = 254 nm), tungsten lamps (λ > 410 nm), and continuously operated xenon lamps (λ = 400–1000 nm) [8]. Several factors can influence the efficacy of the radiation system, including wastewater characteristics, UV intensity, microbe exposure period to UV, and the reactor design [39].

Continuous-wave mercury vapor lamps are commonly used in photochemical AOPs, in which the lamps are arc discharge instruments that emit UV radiation by creating an electric arc between the two electrodes in specifically constructed lamps containing mercury vapor or a combination of mercury and another gas [40]. The energy released by the excitation of the mercury vapor results in the emission of UV radiation. However, there are concerns over mercury toxicity, high energy needs, mechanical instability, and the cleaning costs of the application of mercury lamps, thus emphasizing the need to find alternative UV sources [33].

5.1. Pulsed UV Lamps

Pulsed UV (PUV) lamps are a non-mercury alternative to mercury vapor lamps. PUV lamps are a method that was initially developed for and has been used extensively in the inactivation of bacteria and viruses and is now utilized in industry to decontaminate the cups used in food packaging [8,41]. PUV is based on the use of xenon lamps and it generates polychromatic high-intensity light in a very short period using high-power electrical pulses [33]. The release occurs in a non-toxic, rare-gas environment and can use flashlamps or surface discharge lamps. PUV lamps are instant-on lights that do not require the warm-up period which is required for mercury vapor lamps and also possess higher efficiency [33]. As PUV contains a significant amount of UV light, a potential application of this technology might be its usage as a part of an AOP for the breakdown of polluting dyes. A few studies to assess the performance of PUV have been conducted on dyes such as MG dye and azo dyes in the UV/H_2O_2 process [8,41].

5.2. Ultraviolet Light Emitting Diodes (LEDs)

A light-emitting diode (LED) is a semiconductor device that emits light in a restricted range using electroluminescence [33]. LEDs are made of non-toxic materials and use less energy than conventional lamps because they convert more energy into light and lose less energy as heat. Furthermore, LEDs are durable and emit only the required wavelengths that will save energy. The small size of an LED may be advantageous in some applications [33]. UV LEDs are considered an efficient technology for water treatment, as LEDs with low wavelengths have been developed.

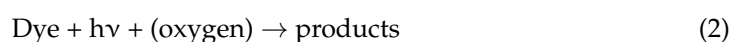### 5.3. Microwaved Electrodeless Discharge Lamp

Microwave-assisted electrodeless discharge lamps also have been widely used and can emit light covering a wide spectrum from vacuum UV to infrared when bombarded with an electromagnetic field [33]. Longer lives are predicted for these lamps since the light lacks an electrode [40]. The microwave power was totally used in the experimental setup to create UV radiation and volumetric heating, both of which contributed to the dye degradation process and resulted in no microwave power energy loss. MWEDL is considered to be effective on an industrial scale for water treatment as well, depending on the reactor configuration [33].

6. Photolysis

Photolysis is termed photodegradation by the irradiation of UV light applied to degrade the compounds that absorb light at shorter wavelengths [22]. The interaction of the light with molecules causes the molecules to degrade into simpler fragments [38]. This method's processes include UV/photolysis, UV/H_2O_2, UV/ozone, and photo-Fenton [22].

6.1. Direct Photolysis

UV/photolysis is a process that uses UV irradiation without oxidants and catalysts to break down the contaminants into smaller molecules [42]. The water molecule is cleaved under UV irradiation and transformed into hydrogen and hydroxyl radicals [20]. The photolysis reaction of dye can be represented by the following equation:

$$\text{Dye} + h\nu + (\text{oxygen}) \rightarrow \text{products} \tag{2}$$

$$H_2O + h\nu \rightarrow {}^{\bullet}OH + H \tag{3}$$

$$\text{Dye} + {}^{\bullet}OH \rightarrow \text{products} \tag{4}$$

6.2. Photolysis Method Based on H$_2$O$_2$ (UV/H$_2$O$_2$)

The UV/H$_2$O$_2$ process is a method that employs hydrogen peroxide in conjunction with UV radiation. Hydrogen peroxide involves external activation, such as UV light, and the photolysis of hydrogen peroxide will produce an effective oxidizing species, hydroxyl radical ($^\bullet$OH) [18]. The generation of hydroxyl radicals by the reaction of UV/H$_2$O$_2$ is as follows:

$$H_2O_2 + h\nu \rightarrow 2^\bullet OH \tag{5}$$

6.3. Photolysis Method Based on O$_3$ (UV/O$_3$)

In the UV/O$_3$ process, the generation of hydroxyl radicals occurs via ozone photolysis in the presence of water [18]:
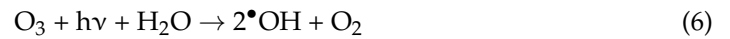
$$O_3 + h\nu + H_2O \rightarrow 2^\bullet OH + O_2 \tag{6}$$

Table 3 shows previous studies on the degradation of dyes via photolysis.

Table 3. Various photolysis processes for degradation of dyes.

Dye	Type of Photolysis	Experimental Conditions	COD/TOC/Degradation Percentage/other Remarks	Reaction Kinetics	Reference
MB—cationic dye, thiazine	UV/H_2O_2	UV light source (UV lamp = 6 W)	- 99.86% of 10 ppm MB with 15 mL of 10% H_2O_2 after 60 min - 99.22% of 20 ppm MB with 15 mL of 30% H_2O_2 for 60 min - 98.90% of 30 ppm MB with 15 mL of 50% H_2O_2 after 90 min)	N/A	[39]
MB	UV	UV lamps (UV-A, UV-B, UV-C)	- COD removal: 83.3% achieved after 60 min (UV-C) - 96.7% degradation of MB after 5 h (UV-C)	First-order	[42]
Blue 13 -monoazo dye	UV/H_2O_2	UV-A (6, 12 and 18 W)	- 0.49–2.43% discoloration with 6 W light intensity - 0.88–4.86% discoloration with 12 W light intensity - 1.26–7.30% discoloration with 18 W light intensity	N/A	[43]
RhB	UV/H_2O_2	$[H_2O_2]$ = 0.10–1020 mg/L, pH 4.5, UV light (low pressure, λ = 254 nm)	- 100% discoloration with 51 mg/L H_2O_2 in 6 min - TOC: 69% reduced	N/A	[44]
RB 19—anionic, anthraquinone	UV, UV/O_3	Two monochromatic germicidal lamps (40 W, 253.7 nm), T = 20 °C, $[RB19]_0$ = 230 $\pm$ 1.5 mg/L, pH 6.0, $[O_3]_0$ = 50 $\pm$ 2 mg/L	- Direct UV photolysis was negligible - TOC: 94% decreased after 120 min	Pseudo-first-order	[28]

Table 3. *Cont.*

Dye	Type of Photolysis	Experimental Conditions	COD/TOC/Degradation Percentage/other Remarks	Reaction Kinetics	Reference
MO	UV	Medium pressure Hg lamp (150 W, 350–400 nm), pH 7.3, $[MO]_0 = 100$ μM	- 45.7% MO degraded after 120 min	Pseudo-first-order	[20]
Basic Red 1 (BR1)—cationic dye	UV/Fenton	Mercury lamp (9.5 W, 254 nm), pH 3.0, $[BR1]_0 = 100$ mg/L	- 90% degraded of BR1 after 60 min - 70% of TOC is removed	N/A	[45]
Brilliant blue FCF (BBF) -Triarylmethane dye, anionic	UV/Cl	Radiation sources: UV lamp (4W, 254 nm, Philips) as UVC source, solar irradiation as an alternative	- Acidic pH is favorable - Solar irradiation is an alternative to UVC lamp - Degradation rate increases when iron and copper are present - After 80 min, 37% of BBF was mineralized	Pseudo-first-order	[46]
Congo red (CR) -Azo dye	UV/NO$_3$	Low-pressure UV (254 nm)	- The degradation rates were 81.90%, 17.46%, and 0.63% by OH$^\bullet$, NO$_2$$^\bullet$, UV radicals respectively - Neutral conditions are favorable	Pseudo-first-order	[47]
MB—Cationic dye	VUV/UV/ Persulfate	$[MB]_0 = 10$ μM, $[PS]_0 = 0.5$ mM, T = 25 °C, Reaction time = 10 min.	- VUV generated more reactive OH$^\bullet$ and SO$_4$$^{\bullet-}$ radicals than a conventional UV/persulfate process. - MB degradation increases with increasing pH solution (3.0–11.0)	N/A	[48]

Dye	Type of Photolysis	Experimental Conditions	COD/TOC/Degradation Percentage/other Remarks	Reaction Kinetics	Reference
Chlorazol black (CB)	UV/acetone	[CB] = 20 mg/L at 25 °C, [Acet.]$_0$ = 50 mM, pH = 3–9	- CB was nearly full degraded after 30 min in the presence of acetone, which was 5.6 times greater compared to UV alone. - Strong alkaline pH is favorable	First-order	[49]
Direct yellow 106 (DY106)—Azo dye, anionic	PL direct photolysis, PL/H$_2$O$_2$	Pulsed light, [DY106]$_0$ = 20 mg/L, [H$_2$O$_2$]$_0$600 mg/L, pH 9.5	- PL direct photolysis was negligible on the degradation due to the highly stable chemical structure of the dye. - PL/H$_2$O$_2$ process reaches 90% of degradation.	Pseudo-first-order	[8]
C.I. Acid Blue 25 (AB25) Anthraquinone	Direct UV irradiation, UV/H$_2$O$_2$, UV/Fe(II)	Direct photolysis: - effect of initial concentration: [AB25] = 10–150 mg/L, pH = 5.7, t = 20 min - Effect of pH: [AB25] = 50 mg/L, pH = 1.4–5.7, t = 20 min	- 100% decolorization for 10 mg/L of AB25 with photolysis. - Degradation rates in acidic solutions (1.4–3) are higher, decreasing from pH 1.4 to 5.7, and there is nearly no change in the pH range of 5.7–9.3. Higher decolorization rates are observed in basic media (10.5–11.8).	Pseudo-first-order	[50]
Reactive orange 16 (RO16)—anionic dye	UV, UV-C/H$_2$O$_2$	UV-C germicidal tubes (8 W), pH = 6.5, t = 30 min	- Degradation by direct photolysis without H$_2$O$_2$ was negligible - Decolorization rate increased with increasing in H$_2$O$_2$	Pseudo-first-order	[51]

Table 3. *Cont.*

Dye	Type of Photolysis	Experimental Conditions	COD/TOC/Degradation Percentage/other Remarks	Reaction Kinetics	Reference
Reactive orange 16 (RO16)—anionic dye	UV, UV-C/H_2O_2	UV-C germicidal tubes (8 W), pH = 6.5, t = 30 min	- Degradation by direct photolysis without H_2O_2 was negligible - Decolorization rate increased with increasing in H_2O_2	Pseudo-first-order	[51]
RO16 -Anionic mono-azo dye	UV/H_2O_2	Low-pressure mercury vapor lamp (28 W, 253.7 nm)	- Neutral conditions are favorable - Decolorization of 50.0 mg dm^{-3} RO16 was completed in <6 min at pH 7, with a UV light intensity of 1950 μW cm^{-2}) - Optimum H_2O_2 concentrations are in a range from 20 to 40 mM	Pseudo-first-order	[52]
RB19	UV, UV/H_2O_2	Low pressure mercury lamp (65 W, 254 nm), $[RB19]_0$ = 10–100 mg/L for photolysis, a fixed $[RB19]_0$ = 100 mg/L and $[H_2O_2]$ = 100,300, 500 and 800 mg/L for UV/ H_2O_2, pH = 3	- Dye degradation with UV photolysis is negligible as the DOC reduction was less than 2% after 300 min. - 91% of RB19 was degraded after 3h of UV/H_2O_2 reaction at a concentration of 500 mg L^{-1} H_2O_2	N/A	[53]
Acid Orange 8 (AO8), Acid blue 29 (AB29), Acid blue 113 (AB113) (Azo dyes)	VUV/H_2O_2	Low-pressure mercury 185 nm vacuum UV lamp (6 W),	- 90% of orange 8, 50% of acid Blue 29, and 60% of acid Blue 113 were degraded after 60 min of irradiation time.	First-order	[54]
Reactive red 120 (RR120)	UV/Fe^3	Low pressure mercury lamp, $[Fe^{+3}]_0$ = 0.25–2.75 mM, $[MB]_0$ = 100–200 mg/L, initial pH 1–11	- 92% color of the dye was removed in 55 min under conditions of Fe^{3+} concentration, 2.35 mM, pH 3.6, and an initial dye concentration of 170 mg/L	N/A	[55]

Dye	Type of Photolysis	Experimental Conditions	COD/TOC/Degradation Percentage/other Remarks	Reaction Kinetics	Reference
Reactive green 19 (RG19)	UV/ H_2O_2	Low-pressure mercury lamp (6 W, 254 nm), pH 2–10, $[RG19]_0$ = 90 mg/L	- Complete decolorization after 20 min - 63% TOC removed in 90 min	Pseudo-first-order	[56]
Acid red 27 (AR27) (anionic dyes)	UV/H_2O_2	Low-pressure mercury lamp (8 W) H_2O_2 (0.03% (*v/v*), $[RG19]_0$ = 50 µg mL^{-1}, sample flow rate of 6 mL min^{-1}	- >99.9% degradation completed with hydroxyl radicals.	N/A	[27]
Basic Fuchsine dye	UV	UV-A light, pH 6.4	- Acidic medium is favorable - Degradation from 73.75% to 89.63% at 70 min	N/A	[57]
Brilliant green (BG)	UV	UV tubes (11 W, 350–450 nm), [BG] = 10–50 ppm	- Higher for the concentrations of 10 (61.5%) and 20 ppm (63.5%) and lower for initial concentrations of 30 (52.9%) and 40 ppm (40.7%).	First-order	[58]
Allura red	UV	T = 35 °C, t = 1–6 h, pH =3–12	- After 1 h of irradiation, 95 % of Allura red (50 ppm) degraded at pH 12 and 35 °C	N/A	[59]
Erythrosine	UV	T = 35 °C, t = 1–6 h, pH =3–12	- After 6 h of irradiation, 90% of Erythrosine (50 ppm) degraded at pH 6 and 30 °C	N/A	[59]
Remazol turquoise blue (RTB)	UV/H_2O_2	UV lamp (6 W, 254 nm), $[RTB]_0$ = 25 ppm	- Under optimum conditions, degradation of the dye could achieve 50% in 10 min - PO_4^{3-}; Cl^-, and CO_3^{2-} increased the degradation rate of the dye	First-order	[60]

Table 3. *Cont.*

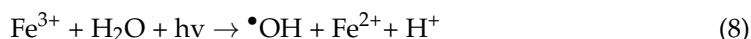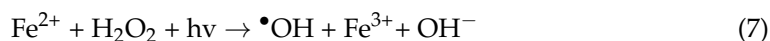| Dye	Type of Photolysis	Experimental Conditions	COD/TOC/Degradation Percentage/other Remarks	Reaction Kinetics	Reference
Acid red 94 (AR94)—xanthene dye	UV/H_2O_2	UV lamp (254 nm),	- Maximum decolorization was 90% with conditions of 0.005 mM dye, at optimum 0.042 M H_2O_2 and pH 6.6.	Pseudo-first-order	[61]
Alizarin yellow (AY)—azo dye	UV/acetone, UV/H_2O_2, UV/$S_2O_8^{2-}$	Low-pressure mercury lamps (15 W, 254 nm), T = 18 °C and 20 °C, pH = 1.7, 2, 11.5 and 12	- The degradation rate of AY for a reaction time 40 min in ascending order: UV/acetone (10^{-2} M, 17%) < UV/H_2O_2/$S_2O_8^{2-}$ (10^{-2} M, 60%) < UV/ $S_2O_8^{2-}$ (10^{-2} M, 81.37%) < H_2O_2/UV (10^{-2} M, 97.68%)	N/A	[62]
Carmine (C.I. natural Red 4)	UV/H_2O_2	UV lamp (254 nm), T = 25 °C, $[dye]_0$ = 20–160 μM, $[H_2O_2]_0$ = 0.83–6.64 mM, pH = 2–10, t = 30 min	- Optimum conditions of 62 μM dye are 5.5 mM H_2O_2 and pH 4.	N/A	[63]
Mordant red 73 (MR73)	UV/H_2O_2	[MR73] = 0.1 mM, 0.05 mM, 0.05 mM, $[H_2O_2]_0$ = 2.5 mM, pH 3 and T = 25 °C	- MR73 decolorization was complete in less than 1 h under optimum conditions. - 65% of MR73 was mineralized after 3 h.	Pseudo-first-order	[64]
Direct red 23 (DR23) AB25 Mordant Orange 1 (MO1)	UV/Fenton	Mercury lamp (9.5 W, 254 nm)	- 32% of TOC and 48% of the color of DR32 was removed after 1 h. - Complete decolorization and more than 90% of TOC for AB25 and MO1.	First-order	[45]
Blue 13 Monoazo dye	UV/ H_2O_2	UV lamp (6,12 and 18 W, 254 nm), Comparing the UV intensity	- 99.70% of dye decolorized at 0.67% H_2O_2 using 18 W intensity of UV light for 40 min at 7.86 pH.	N/A	[43]

Dye	Type of Photolysis	Experimental Conditions	COD/TOC/Degradation Percentage/other Remarks	Reaction Kinetics	Reference
MG, Bromocresol purple (BCP)	UV	Low-pressure mercury lamp (15 W, 254 nm), T = 18–20 °C, pH 5.8 for MG and pH 4.5 for BCP	- 25% of BCP degraded and 66% of MG degraded after 240 min.	Pseudo-first-order	[65]
Orange G Azo dye, anionic	UV, UV/acetone, UV/H_2O_2, UV/$S_2O_8^2$	Low-pressure mercury lamp (15 W, 254 nm), T = 18–20 °C, pH 5.8 for MG and pH 4.5 for BCP	- The results obtained from direct photolysis of the dye were negligible. - Complete decolorization by UV/acetone after 1 h.	N/A	[66]
RhB—xanthene	UV, UV H_2O_2, UV/Persulfate	Medium-pressure mercury lamp (330 W, 365 nm)	- With only UV irradiation, the degradation of RhB reached 45% after 6 min. - 96% and 87% of RhB were removed by the UV/H_2O_2 and UV/PS processes, respectively, after 15 min. - TOC removal was 50% by UV/H_2O_2 process and 60% by UV/PS process.	Pseudo first order	[67]
Reactive black 5 (RB5)—anionic dye	UV, UV/H_2O_2	Low-pressure mercury lamp (55 W), [RB5]$_0$ = 10–50 mg/L, t=120 min	- 60% decolorization was achieved after 120 min at 50 mg/L of RB5 with UV irradiation.	Pseudo-first-order	[68]
Disperse orange 25—non-ionic	UV, UV/H_2O_2	Low-pressure mercury lamp (55 W), [RB5]$_0$ = 10–50 mg/L, t = 120 min	- Low photodegradation rate because of low aqueous solubility (non-ionic dye). - Only 10.6% decolorisation was achieved after 120 min	Pseudo-first-order	[68]

Table 3. *Cont.*

Dye	Type of Photolysis	Experimental Conditions	COD/TOC/Degradation Percentage/other Remarks	Reaction Kinetics	Reference
Basic blue 3 (BB3), Acid green 25 (AG25)	UV/ H_2O_2	Mercury lamp (30 W, 254 nm), pH 6.5, $[H_2O_2]_0$ = 1.2 g/L, $[BB3]_0$ = 10 mg/L, $[AG25]_0$= 10 mg/L	- BB3 achieved 95.03% of removal after 20 min - AG25 achieved 98.16% of removal after 20 min	Pseudo-first-order	[69]
MO	UV/ H_2O_2	UV lamp (254 nm), $[MO]_0$ = 7.80 × 10^{-5} M, $[H_2O_2]_0$ = 4.58 × 10^{-2} M	- Complete degradation of 0.078 M of MO after 3 min and only 26% degradation of MO after 4 h without H_2O_2	Pseudo-first-order	[70]
MB	UV/ H_2O_2	Medium pressure lamp (300 W, 365 nm),	- Optimum pH and H_2O_2 dosage of the photolysis process were pH 4–5 and 0.165 mL 30% H_2O_2 per mg of MB.	First-order	[71]
Tartrazine	UV	Solar UV, UV lamp (24 W, 365 nm), t = 300 min, flow rate of solution = 60 mL/s, $[dye]_0$ = 10 mg/L, pH 8.2–8.5	- 2% of dye was degraded after 300 min.	N/A	[72]
Indigo carmine	VUV	VUV light from Xe-Ne plasma (147–172 nm),	- No oxidizing agent or catalyst is required	N/A	[73]

6.4. Photo-Fenton

Photo-Fenton is a process utilizing the combination of UV radiation with Fenton's reagents (solution of hydrogen peroxide with ferrous iron), and as the light irradiation increases, the Fenton process efficiency will also increase. Irradiation with UV light could speed up the degradation of organic pollutants. The reactions of photo-Fenton are shown in Equations (7)–(9). UV light causes not only the production of more hydroxyl radicals but also the reuse of ferrous catalysts through Fe^{3+} reduction (Equation (8)) [45]. The decomposition of $Fe(OH)^{2+}$ also enhances more $^{\bullet}OH$ radicals (Equation (9)) [18]:

$$Fe^{2+} + H_2O_2 + h\nu \rightarrow {}^{\bullet}OH + Fe^{3+} + OH^- \tag{7}$$

$$Fe^{3+} + H_2O + h\nu \rightarrow {}^{\bullet}OH + Fe^{2+} + H^+ \tag{8}$$

$$Fe(OH)^{2+} + h\nu \rightarrow Fe^{2+} + {}^{\bullet}OH \tag{9}$$

7. Factors Affecting the Degradation Rate of Photolysis Methods

7.1. Contact Time

Previous studies have reported that dye concentration in aqueous solutions decreases with irradiation exposure time. Joseph et al. [42] have reported that MB concentration degraded more with longer irradiation time. Safni et al. [74] have also reported that the degradation percentage of orange F3R by photolysis increased with increasing irradiation time with or without catalysts. This is because the longer the UV irradiation time, the more energy is absorbed by dye molecules from photons which facilitate them to degrade. The degradation efficiency also increases with irradiation time, because more hydroxyl radicals can be generated to oxidize the organic pollutants to break down into simpler molecules [42,74].

7.2. Radiation Source

Primarily, artificial light sources are purposely used in the photolysis process in wastewater treatment to maintain stable intensities and avoid other environmental factors. The intensity and wavelength of the light source significantly affect the photodegradation rate [34]. A shorter wavelength gives higher-energy photons, which will increase the degradation efficiency [42]. The higher intensity means more photons can be absorbed to generate hydroxyl radicals. However, in most photolysis experiments, very high-intensity light is avoided due to the probability of temperature rise, which could cause a thermal reaction [34]. The effects of UV irradiation intensities have been studied by Jamal et al. [43] and Algubili et al. [75]. They reported that the degradation percentage of dyes increased after treatment with increasing intensities of UV irradiation. The effect of different types of UV irradiation has been proven by Joseph et al. [42], who found that between four types of irradiation, UV-C (254 nm), UV-B (311 nm), UV-A (365 nm), and a solar lamp (610 nm), UV-C degraded MB dye almost 80% in only 1 h compared to after 5 h using UV-B, UV-A, and solar, which were only 12.07, 38.24, and 29.56, respectively.

7.3. pH of the Medium

The pH of the medium plays a vital role as a parameter of the degradation efficiency of dyes due to the wide range of pH values of dye effluents. In previous studies, researchers have performed comparative experiments on different pH conditions in the photochemical process. Ghodbane and Hamdaoui [50] have reported that the degradation rate of AB25 in acidic solutions (1.4–3) is higher, decreases from pH 1.4 to 5.7, and there is nearly no change in the pH range of 5.7–9.3. Then, higher decolorization rates were observed in a basic solution (10.5–11.8) because of the higher facility of OH radicals generated at these pH values. Mullapudi et al. [27] have reported that the maximum degradation of AR27 and MB by UV/H_2O_2 was achieved in the pH range of 3–9. The efficiency of degradation was decreased when the pH of the solution increased from 10 to 11. It can be explained that at higher pH, H_2O_2 deprotonates to form hydroperoxy anion (HO_2^-) which is a conjugate

base of H_2O_2. The formed hydroperoxy anion reacts with OH^- radicals and H_2O_2, yielding dioxygen and water, thereby reducing the availability of hydroxyl radicals to attack the target molecule and affecting the degradation efficiency [41].

$$OH^- + HO_2^- \rightarrow H_2O_2 + O_2^- \tag{10}$$

$$H_2O_2 + HO_2^- \rightarrow H_2O + O_2 + OH \tag{11}$$
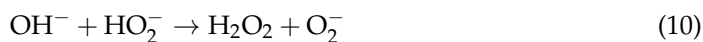
7.4. Initial Concentration of Dyes

Many researchers have performed photolytic experiments by varying the initial concentration of dyes to investigate the effects on the degradation of dyes and organic pollutants. It is proven that the higher the initial concentration of dye, the lower the degradation rate. At high concentrations, the penetration of photons entering the solution diminishes, resulting in an inner filter effect and the solution is not accessible by UV light [75,76]. Bendjama et al. [49] have reported that the degradation efficiency of CB dye decreased with increasing initial concentration. For example, complete degradation was achieved for a dye concentration of 5 mg/L, and the result observed decreased to about 95% for 20 mg/L, 80% for 30 mg/L, and 37.4% for 50 mg/L of CB. Ghodbane and Hamdaoui [50] also reported that the degradation rate of AB25 dye decreased with an increasing initial concentration of dye. Similarly, it was also reported by Soltani and Entezari [77] that the photocatalytic degradation of MB dye is affected by the initial concentration, as the degradation rates were decreased when the initial concentration of MB was increased.

8. Photocatalysis

Photocatalysis is a heterogenous AOP using light irradiation and a semiconductor photocatalyst that absorbs light, which differs from other treatment techniques because this process performs oxidation and reduction simultaneously [22,78]. There are many semiconductor materials that have been used as catalysts for the degradation of organic pollutants and dyes, including TiO_2, ZnO, Fe_2O_3, SnO_2, ZrO_2, CdS, ZnS, and many more. A number of studies have demonstrated that photocatalysis is a reliable and efficient method for degrading dyes in water. Table 4 lists the photocatalytic dye degradation used in the previous literature.

Table 4. Various photocatalysts studied for the degradation of dyes.

Dye	Photocatalyst	Experimental Conditions	COD/TOC/Degradation Percentage/Remarks		Reaction Kinetics	Reference
MB	Ferrite Bismuth nanoparticles	Direct solar irradiation; $[MB]_0 = 15$ mg/L; acidic medium; photocatalyst (0.5 g/L)	-	95% of MB was degraded after 80 min	Pseudo-first-order	[77]
RB5	TiO_2	Low-pressure Hg UV-C lamp (15 W, 254 nm); $[TiO_2]_0 = 0.5$ g/L; $[RB5]_0 = 25–125$ mg/L; pH 6.4–6.9	-	82% TOC and 76% COD removal were achieved after 210 min	Pseudo-first-order	[79]
Procion Blue HERD (PBH)	TiO_2 and ZnO	UV lamp (30 W); $[PBH]_0 = 10–100$ ppm; photocatalyst loading = 0.5–2 g/L; pH 2–10	-	100% decolorization of dye with ZnO at pH 7 and with TiO_2 at pH 4.	First-order	[80]
Methyl orange (MO)	Ag-doped titania-silica	Medium-pressure Hg lamp (150 W, 350–400 nm); $[MO]_0 = 100$ μM; pH 7.3; T = ~20 °C; 0.15 g catalyst	-	After 30 min, photolysis (45.7%) degraded more than photocatalysis.	Pseudo-first-order	[20]
Orange F3R	C-N-codoped TiO_2	UV (10 W, 365 nm), visible (13 W), solar irradiation; $[dye]_0 = 30$ mg/L; dosage of C-N-codoped TiO_2 is 3–15 mg	- - - -	39.05% degraded under UV light after 180 min 40.86% degraded under visible light after 180 min 64.12% degraded under solar light with 6 mg catalyst after 180 min 11.82% without catalyst and the degradation rate increased to 39.05% with C-N-codoped TiO_2	N/A	[74]
MG	TiO_2	UV lamp (15 W, 365 nm); $[MG]_0 = 40$ mg/L; 20 mg of TiO_2	-	99.9% MG degraded after 1 h.	N/A	[81]
Remazol Brilliant Blue (RBB)	ZnO	High-pressure Hg lamp (125 W, 365 nm), $[ZnO] = 1.5$ g/L, $[RBB]_0 = 100$ mg/L	-	100% degradation of RBB	Pseudo-first-order	[75]

Table 4. *Cont.*

Dye	Photocatalyst	Experimental Conditions	COD/TOC/Degradation Percentage/Remarks	Reaction Kinetics	Reference
MB	ZnO/PDMS	Three different types of light sources such as halogen (100 W), metal-halide (150 W), and UV (4 W) light sources.	The highest degradation of MB achieved was 93% under UV/Vis irradiation after 3 h.	N/A	[26]
Rhodamine B (RhB)	TiO_2	Low-pressure UV lamp (15 W, 254 nm), 120 mg TiO_2, pH 4.5, $[RhB]_0 = 5$ mg/L	Color removal achieved 29% after 60 min and TOC, 25%	Pseudo-first-order	[44]
RO16—anionic monoazo dye	UV-C/TiO_2 and UV-C/H_2O_2/TiO_2	UV-C germicidal tubes (8 W), pH 6.5	- UV-C/H_2O_2 is the most effective process compared to UV/TiO_2 or UV/H_2O_2/TiO_2.	Pseudo-first-order	[51]
MO, RhB, MB	Ag-doped titania-silica	Medium-pressure mercury lamp (150 W, 350–400 nm), Catalyst was prepared by sol-gel, catalyst loading is 0.15 g, T = 20 °C	- The degradation rate of MO by photolysis was higher than photocatalysis - The degradation of (RhB) by photocatalysis was higher than photolysis, after 30 min	Pseudo-first-order	[20]
Violet-3B	C-N-codoped TiO_2	Visible-halogen lamp (500 W), $[dye]_0 = 5$ mg/L, catalyst dosage is 0.3 g/L, pH 5.6	- The degradation of violet-3B with visible light and catalyst after 4 h achieved 96% color removal and, due to mineralization, 44% TOC was removed.	Pseudo-first-order	[82]
Tartrazine	UV/TiO_2, UV/H_2O_2/TiO_2	UV lamp (6 W, 254 nm), $[dye]_0 = 2 \times 10^{-5}$ to 8×10^{-5} M, pH 2.2–11, 0.02–0.18 mg/L catalyst dosage, T = 30 °C	- The optimum conditions for the degradation of dye were 6×10^{-5} M dye concentration, pH of 11, and 0.18 mg/L of catalyst dose. - The most effective degradation of the dye was achieved with the combination of UV/H_2O_2/TiO_2	Pseudo-first-order	[83]

Dye	Photocatalyst	Experimental Conditions	COD/TOC/Degradation Percentage/Remarks	Reaction Kinetics	Reference
MG	ZnO–TiO$_2$/clay	UV-A lamp (100 W, 365 nm), catalyst dosage = 1 g, [dye]$_0$ = 75 mg/L, pH 5.2	- Nearly complete mineralization was achieved after 30 min.	Pseudo-first-order	[84]
MG	TiO$_2$ dip-coating	UV lamp, solar irradiation,	- Complete removal in the presence of catalyst after 6 h of sunlight irradiation - 92.15%, 94.28% and 98.43 % for 5, 10 and 15 g of catalysts respectively	Pseudo-first-order	[85]
AO8, AC29, AB113 (Azo dyes)	VUV/TiO$_2$	Low-pressure Hg lamp (18 W, 185 nm), TiO$_2$ dosage = 0.5 g/L, [dye]$_0$ = 0.0523 mM, T = 25 °C, pH 3, 5, 7, 9 and 11	- Degradation of the dyes is more efficient under an acidic medium	Pseudo-first-order	[54]
MB	TiO$_2$, Sn–F/TiO$_2$ NPs	Sol-gel method, UV, and visible light irradiation	- Under UV irradiation, the degradation efficiency of MB was 72% and 91% for TiO$_2$ and Sn-F/TiO$_2$ NPs, respectively - Under visible light, the degradation efficiency was 91.6% and 94.4% for TiO$_2$ and Sn-F/TiO$_2$ NPs, respectively	Pseudo-first-order	[86]
RB5—anionic dye	TiO$_2$	UV lamps (40 W, 365 nm), pH (3–11), catalyst load (0.5–3.0 g/L), and [RB5]$_0$ = 20–100 mg/L	- Maximum degradation rate of 26.5 mg/g of dye after 30 min was at pH 3 and a catalyst load of 1.5 g/L - TOC reduced by 70%	Pseudo-first-order	[87]
MB—cationic dye	TiO$_2$, TiO$_2$ ENR	Fluorescent lamp,	- Alkaline medium was favourable	Pseudo-first-order	[88]

Dye	Photocatalyst	Experimental Conditions	COD/TOC/Degradation Percentage/Remarks	Reaction Kinetics	Reference
MB	TiO_2	UV-A, UV-B, UV-C and solar light, $[MB]_0$ = 2–10 ppm, pH (4–10), t = 1 h.	- Complete degradation of MB was achieved within 14 min with UV-C irradiation, 18 min with UV-B irradiation, and 20 min with UV-A irradiation	First-order	[89]
RB5—azo dye	ZnO, TiO_2	Catalyst load = 0.5–1.5 g/L, $[RB5]_0$ = 25–150 mg/L), pH = 3.0–11.0	- The color removal efficiencies of RB5 were 99.8% and 58.1% using ZnO and TiO_2 after 60 min. - Rapid color removal with pH between 3 and 9	Pseudo-first-order	[90]
RB5	TiO_2, ZnO	UV lamp (20 W, 365 nm), Catalyst load = 1.25 g/L, $[RB5]_0$ = 10–100 mg/L), pH = 3.0–11.0	- Complete decolorization with ZnO and 75% decolorization with TiO_2 after 7 min - Acidic medium is preferred.	Pseudo-first-order	[91]
Reactive orange 4 (RO4)	TiO_2, ZnO	UV lamp (20 W, 365 nm), Catalyst load = 1.0 g/L, $[RO4]_0$ = 10–100 mg/L), pH = 3.0–11.0	- 92% decolourization with ZnO and 62% decolorization with TiO_2 after 7 min	Pseudo-first-order	[91]
MB—cationic	Ta-doped ZnO	Xe arc lamp (300 W), $[MB]_0$ = 10 mg/L, 50 mg, pH 8	−1 mol% Ta-doped ZnO annealed at 700 °C exhibits the highest degradation rate.	Pseudo-first-order	[92]
AO7	TiO_2	High-pressure mercury lamp (400 W)	- Complete removal of 0.086 mM AO7 after 20 min at pH 6.8	First-order	[93]
Reactive red	TiO_2	High-pressure mercury lamp (400 W)	- Complete removal of 0.086 mM of RR2 after 20 min at pH 6.8	First-order	[93]

Dye	Photocatalyst	Experimental Conditions	COD/TOC/Degradation Percentage/Remarks	Reaction Kinetics	Reference
Reactive red	TiO_2	High-pressure mercury lamp (400 W)	- Complete removal of 0.086 mM of RR2 after 20 min at pH 6.8	First-order	[93]
Procion yellow H-EXL	N-doped TiO_2	UV lamp (100 W)	- Optimum conditions were found to be at pH 5 with a TiO_2 dosage of 1 g/L.	N/A	[94]
Tartrazine—anionic azo dye	TiO_2	Solar UV, UV lamp (24 W, 365 nm), t = 300 min, flow rate of solution = 60 mL/s, $[dye]_0$ = 10 mg/L, TiO_2 dosage = 0.3 mg/cm^2, pH 8.2–8.5	- The removal efficiency was 97% for the solar reactor and 30% for the lamp reactor. - Acidic medium is preferred.	N/A	[72]
CV, Methyl red (MR), Basic blue (BB)	ZnO, TiO_2, SnO	Solar irradiation, $[dye]_0$ = 10 mg/L, pH 9	- COD removal: 92% for CV, 95% for BB, and 89% for MR after 5 h irradiation with the presence of ZnO.	N/A	[95]
MG	ZnS, Mn-doped ZnS	Medium-pressure lamp (125 W), pH 2–5, t = 90 min, $[MG]_0$ = 25 g/L	- Degradation efficiency increased from 60 to 72% as the pH increased from 2 to 4	Pseudo-second-order	[96]
Reactive red 4 (RR4)	TiO_2, N-doped TiO_2	LED light irradiation, $[RR4]_4$ = 30 mg/L, 0.030 g catalyst	- Complete degradation of RR4 after 60 min with N-doped TiO_2 - 40% of RR4 was removed by undoped TiO_2 after 30 min and no change thereafter.	N/A	[97]
MB	SnO	Low-pressure mercury lamp (125 W, 254 nm), 0.02 g SnO_2, $[MB]_0$ = 10 mg/L,	- No degradation by visible light. - Complete degradation with UV irradiation after 30 min with SnO.	First-order	[98]

Dye	Photocatalyst	Experimental Conditions	COD/TOC/Degradation Percentage/Remarks	Reaction Kinetics	Reference
MB, RB	Fe-doped NiO	Sunlight radiations, $[RB]_0 = 5$ ppm, $[MB]_0 = 5$ ppm, t = 60 min,	- 86% of RB was degraded and 85% of MB was degraded after 60 min.	Pseudo-first-order	[99]
MB	Ni-doped ZrO_2	Visible light lamp (>400 nm), $[dye]_0 = 5$ ppm, 15 mg of photocatalyst	- 92.2% degradation of dye after 100 min under visible light irradiation.	Pseudo-first-order	[100]
MB, MO	Pd-doped TiO_2	High-pressure lamp (100 W), $[MB]_0 = 20$ mg/L, $[MO]_0 = 20$ mg/L,	- Without catalyst, 15.6% of MB and 87.8% of MO degraded under irradiation after 120 min. - Complete decolorization for both MB and MO after 120 min.	Pseudo-first-order	[101]
MB	Co-doped TiO_2	UV-C lamp, $[MB]_0 = 10$ ppm, 0.5 g/L catalyst	- Without a catalyst, 1.3% of MB was degraded after 100 min. - 81.4% degradation of MB with catalyst after 100 min	Pseudo-first-order	[102]
RB	ZnO nanoparticles	UV lamp (15 W, 256 nm), 0.05 g ZnONPs, $[dye]_0 = 20$ mg/L, pH 4,8 and 11	96, 100 and 83% of RB degraded at pH 4, 8 and 11 respectively after 240 UV irradiation	First-order	[103]
MB	Immobilised TiO_2	$[MB]_0 = 75$ mg/l, [Zinc] = 60 mg/L, [NaCl] = 0.250 M, flowrate of 0.7 L/min.	After 180 min of UV radiation, a 79.27% reduction in initial dye concentration was observed.	N/A	[104]

8.1. Photocatalysts

8.1.1. Titanium Dioxide, TiO_2, and Metal Oxide Semiconductors

Among the various photocatalysts, TiO_2 is practically the only material appropriate for industrial applications at the moment and, most likely, in the future. This is due to the fact that TiO_2 has the most efficient photoactivity, the best stability, and is inexpensive and readily available [44,78]. TiO_2 degrades well-known cationic dyes such as MB, MG, MR, and basic violet. Basic dyes with high molecular weight are vulnerable to $OH^\bullet$ and radicals produced by TiO_2 [105]. Other than TiO_2, metal oxide semiconductors such as SnO_2, ZnO, NiO, ZrO_2, and ZnS have been used as photocatalytic materials. Among the metal oxides, ZnO has also been utilized as a photocatalytic material in wastewater treatment for decolorization It is low-cost, chemically stable, and has a larger light absorption spectrum than TiO_2 [105].

8.1.2. Modifications to Enhance Photocatalyst Activity

Metal Doping

The drawback of using TiO_2 as a photocatalyst is that it can be operated only under UV irradiation (250 nm–350 nm) [105]. Because of the magnitude of its band gap energy (3.0–3.3 eV), TiO_2 absorbs only a small percentage of the solar spectrum radiation [106,107]. In order to enhance the photocatalytic activity of TiO_2, the researchers make nanocomposites with metal and non-metal because it can be enhanced by decreasing the unwanted recombination of photoinduced holes and electrons and expanding the catalyst's photo response to the visible light area [108]. Metal ions such as manganese (Mn), zinc (Zn), aluminum (Al), iron (Fe), nickel (Ni), silver (Ag), palladium (Pd), chromium (Cr), vanadium (V), and platinum (Pt) have been widely used for doping with catalysts in order to minimize the band gap energy, which will improve the efficiency of UV light photocatalysis [108]. However, metal doping was also reported to have thermal instability and an increase in carrier trapping, which may decrease the photocatalytic efficiency [106]. Tolia et al. [96] have investigated the photocatalytic degradation of MG dye using Mn-doped ZnS and undoped ZnS nanoparticles. They found that with the doped photocatalyst, the rate of decolorization was increased as the Mn ion also functions as an oxidizing agent. However, it was discovered that increasing the doping concentration decreases photodegradation efficiency because the increase in manganese ions replaces Zn ions in the ZnS lattice structure and creates MnS, which reduces the activity of trapping electrons or holes.

Non-Metal Doping

Doping with non-metal also can enhance the efficiency of photocatalysis by suppressing electron-hole recombination and increasing the redox potential of $OH^\bullet$. Non-metal materials that have been utilized for doping are S, C, B, N, P, I, and F [109]. The inclusion of a co-dopant in photocatalysis can result in fast recombination of hole-electron pairs, implying that co-dopant TiO_2 has greater photocatalytic degradation efficiency than single dopant TiO_2. However, too much TiO_2 doping would be unfavorable to the photocatalytic activity of the photocatalyst. Thus, an optimal amount of dopant is utilized to optimize the effectiveness of the photocatalytic activity [108]. Nitrogen doping onto TiO_2 is considered due to high stability, small ionization, and comparable atomic size with oxygen that is better than standard TiO_2 and shows improved photocatalytic activity in the visible region [107]. In the photocatalysis of reactive red 4 (RR4), complete degradation was observed with N-doped TiO_2 after 60 min of LED light irradiation compared to only 40% or RR4 dye removed by undoped TiO_2 [97]. The result clearly demonstrated that the N element in TiO_2 lowered the band-gap energy, resulting in the photocatalyst being active under low visible light energy.

8.2. Mechanism of Photocatalysis

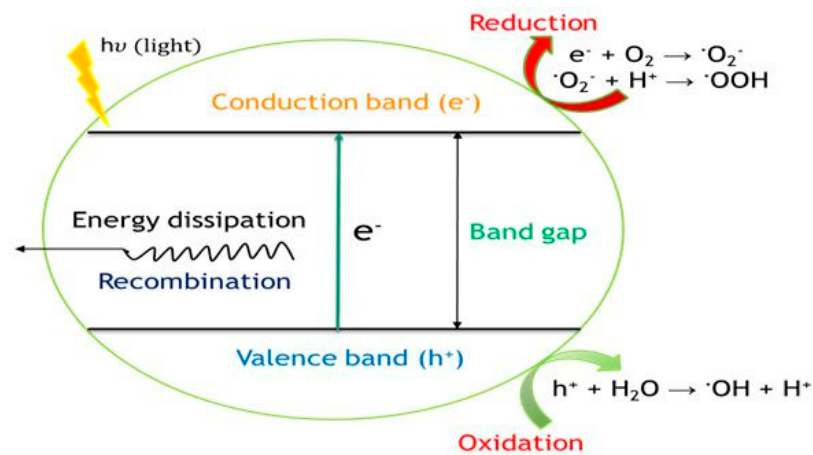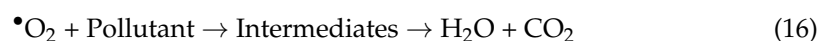The schematic diagram of the general mechanism of photocatalysis is illustrated in Figure 2.
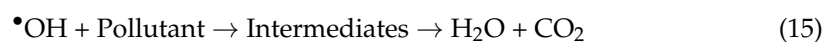
Figure 2. Schematic diagram of the mechanism of photocatalysis. Source: Mishra et al. [78].
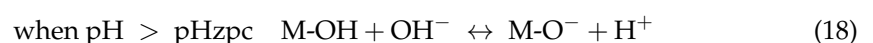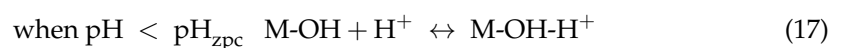
The transport of pollutants from the surrounding environment to the photocatalyst surface is the first step in photocatalysis. The dye compounds are initially adsorbed onto the surface, where oxidation and reduction reactions take place [105]. The photocatalyst usually has band structures that include an empty conduction band and a filled valence band. When light strikes a semiconductor, its energy photons exceed the semiconductor's energy gap, and electrons are excited from the valence band to the conduction band by leaving holes behind (Equation (12)) [78]. The activated holes in the valence band (h_{VB}^+) react with water, generating hydroxyl radicals ($^\bullet$OH) (Equation (13)) and electrons in the conduction band (e_{CB}^-), generating superoxide radicals (Equation (14)) [78]. These radicals then degrade the pollutants into intermediates and further degrade to obtain H_2O and CO_2 (Equations (15) and (16)) [22]. The products are then desorbed from the surface of the photocatalyst and moved back into the aqueous phase [105]. The summarized reactions in the photocatalysis process are as follows:

$$\text{Photocatalyst} + h\nu \rightarrow h_{VB}^+ + e_{CB}^- \tag{12}$$

$$H_2O + h_{VB}^+ \rightarrow {}^\bullet OH \text{ (hydroxyl radical)} + H^+ \tag{13}$$

$$O_2 + e_{CB}^- \rightarrow O_2 \text{ (superoxide radical)} \tag{14}$$

$${}^\bullet OH + \text{Pollutant} \rightarrow \text{Intermediates} \rightarrow H_2O + CO_2 \tag{15}$$

$${}^\bullet O_2 + \text{Pollutant} \rightarrow \text{Intermediates} \rightarrow H_2O + CO_2 \tag{16}$$

8.3. Factors Affecting Photocatalysis Process on Degradation of Dyes
8.3.1. Effect of pH

The key mechanism of the adsorptive removal of dyes in an aqueous solution is electrostatic interactions between dyes and metal catalysts. Metal hydroxyl groups (M-OH) are formed as a result of the adsorption of H_2O molecules and the dissociation of OH^- groups at the metal surface. When the solution pH is lower than the zero-point charge (ZPC) of the photocatalysts, the surface is positively charged (Equation (16)). On the other hand, when the solution pH is greater than the ZPC of the photocatalysts, the surface is negatively charged (Equation (17)) [5,88,89]. A high adsorption capacity is observed when anionic or cationic dyes are adsorbed on the photocatalyst surface at acidic or basic pH [5].

$$\text{when pH} < \text{pH}_{zpc} \quad \text{M-OH} + H^+ \leftrightarrow \text{M-OH-}H^+ \tag{17}$$

$$\text{when pH} > \text{pHzpc} \quad \text{M-OH} + OH^- \leftrightarrow \text{M-O}^- + H^+ \tag{18}$$

Laohaprapanon et al. [90] reported that the rapid color removal rates of RB5 under pH 3–9 were related to the photocatalytic activity of ZnO (pH_{zpc} = pH 9). This can be

explained on the basis of the electrostatic interactions between the anionic dyes with the positive catalyst surface of ZnO under lower pH. However, they also reported that the highest color removal rate was found at pH 11 due to direct dye photolysis and the photocatalytic activity of ZnO. Although lower adsorption at high pH, the possible reason is due to the fact that more hydroxyl radicals are generated from a high concentration of hydroxyl ions. A similar result has been reported by Kansal et al. [91] for RB5 and RO4. Juang et al. [93] also reported that an acidic medium is favorable for the photodegradation process of AO7 and RR2. Jawad et al. [88] reported that MB, which is basically a cationic dye, has the highest photocatalytic efficiency by TiO_2 (pH_{zpc} = pH 6.8) in an alkaline medium. This is because, at high pH, the TiO_2 surface is negatively charged, which causes more adsorption on the catalyst surface due to electrostatic interaction, and also more hydroxyl radicals are generated because more hydroxyl ions are available on the surface.

$$TiOH \leftrightarrow TiO^- + H^+ \tag{19}$$

8.3.2. Effect of Photocatalyst Loading

The photodegradation of dye increases as the amount of the photocatalyst increases. With increasing catalyst concentration, the number of active sites on the surface of the photocatalyst also increases. As a result, the production of OH radicals is increased, which is responsible for the degradation of dye solution [35]. Putri et al. [82] investigated the effect of photocatalyst—C-N-codoped TiO_2—dosage on the degradation of violet-3B. They found that the removal percentage of the dye was increased up to 83% as the catalyst dosage increased up to 0.3 g/L. However, the removal percentage was decreased when the dosage was more than 0.3 g/L, which is due to the increased turbidity of the dye solution which results in the lower penetration of light and increased light scattering [105]. Similar results were reported by Gupta et al. [83] in photocatalysis of tartrazine dye using TiO_2, wherein, by increasing the catalyst dosage from 0.02 g/l to 0.18 g/L, the degradation rate was increased, and then, with a catalyst dose of more than 0.18 g/L, the degradation remained constant. They also explained that when the amount of catalyst increases, the total active surface also increases. Simultaneously, UV-light penetration and the photoactivated volume of the suspension will be reduced due to the high dosage of the photocatalyst.

9. Energy Consumption and Cost–Benefit Analysis

UV-based processes for water treatment depend on the energy consumption in which electrical energy consumption represents a large amount of energy used. As a result, the decreased energy consumption would result in a larger yield and more accessibility of the approach. The amount of electrical energy consumed is determined by a variety of parameters, including the light source, the structure of the pollutants, and the type of reactor used [110]. Since electrical energy is so crucial in AOPs, the IUPAC has proposed a standard for addressing electrical energy used and reaction yield in UV-based AOPs [111].

$$Electrical\ energy\ consumption,\ E_{EO}\ (kWh) = \frac{1000 \times P \times t}{60 \times V \times log\frac{C_0}{C_t}} \tag{20}$$

where P is the power of the used light source (*kW*), t is irradiation time (min), V is the volume of experimented solution (l), C_0 and C_t are the initial and final concentrations of contaminants. E_{EO} is the amount of energy required to degrade the pollutant's concentration in 1 m^3 volume (*kWh*).

Mohajerani et al. [13] stated that UV/H_2O_2 operation normally has a fixed cost of $58,000 and the cost of the UV lamp is $15,000 per year for a treatment plant. T The reduction in the number of UV lamps and reactors needed for the effective treatment of wastewater by the presence of H_2O_2 and increasing the dose of H_2O_2. An economic analysis of photocatalysis has been studied by Raju et al. [112], by comparing the cost of the process of UV alone, UV-TiO$_2$, granular activated carbon (GAC) alone, UV-GAC, and UV-GAC-TiO$_2$. The analysis of the cost is in terms of US Dollars (USD) per kilogram (kg)

of total volatile solids (TVS) utilized by the experimental results using the Equations (20) and (21).

$$Total\ power\ consumed,\ (kWh) = \frac{Power\ used\ (W) \times Reaction\ time\ (min)}{(1000 \times 60)} \quad (21)$$

$$Total\ operation\ cost\ \left(\frac{USD}{kg}\right)$$
$$= \frac{Total\ power\ consumed\ (kWh) \times Unit\ cost\ of\ power\ \left(\frac{USD}{kWh}\right)}{(C_0 - C_F)\left(\frac{mg}{l}\right) \times Working\ volume\ (l)} \times 10^6 \left(\frac{mg}{kg}\right) \quad (22)$$

where C_0 is the initial concentration of TVS, C_F is the final concentration of TVS, and the total power consumed involves the power consumed for the peristaltic pump and/or UV lamps and operating the stirrer. Among the processes, they concluded that UV-GAC-TiO$_2$ photocatalysis is the most cost-effective for wastewater treatment under batch and continuous operations.

10. Reaction Kinetics Model

In the process of photolysis, kinetic studies indicate the information on the optimum conditions for the degradation of dyes such as the initial concentration of dyes. The degradation kinetics of dyes can be determined by regressing the data obtained for the first-order kinetic Equation (22), pseudo-first-order kinetic Equation (23), second-order kinetic Equation (24), and pseudo-second-order kinetic equation Equation (25) [113]. The kinetic orders are being calculated to determine which order will fit the experimental data the best.

$$ln\ A_t = ln\ A_0 - k_1 t \quad (23)$$

$$ln\ (A_t - A_e) = log\ (A_t - A_e) - k_1(2.303)t \quad (24)$$

$$1/A_t = 1/A_0 + k_2 t \quad (25)$$

$$t/A_t = 1/(k_2 A e^2) + (1/Ae)t \quad (26)$$

where A_0 is the initial absorbance of the dye (A), A_t is the effluent absorbance of the dye at time t, A_e is the equilibrium absorbance of the dye, and k_1 (min^{-1}) and k_2 (A^{-1} min^{-1}) are the rate constants of the first-order and second-order kinetic equations [113]. Multiple studies of the photodegradation of dyes have been proven to be fitted to first-order reactions and pseudo-first-order reactions.

A mathematical model was studied under the heterogeneous photocatalytic degradation of wastewater containing petroleum [114]. The various parameters influencing the mechanism of degradation, such as the mass transfer step, the kinetics of the mineralization, etc., were considered as the model parameters. Mass balances were chosen as the bulk region and the catalyst phase was considered as the solid phase in order to develop the model. The degradation mechanism of the solid phase was considered in two stages, such as an equivalent intermediate (EI), in which the toluene is transformed to EI, and in the second stage, the oxidation of EI gives carbon dioxide (CO$_2$). The results found a good correlation between modeling and empirical data in terms of degradation and mineralization. The simulation of the degradation kinetics of the target pollutant was obtained in the absence of a reaction pathway. A good similarity with the experiment was obtained for the target pollutant from the model.

11. Conclusions

One of the reasons for water pollution is the discharge of dye effluent into water bodies. Dye effluents in wastewater must be treated using efficient dye removal processes before being released into the environment, as they are one of the causes of water pollution. It was confirmed that AOPs that facilitate the combination of ultraviolet irradiation, catalysts, and oxidants to produce hydroxyl radicals ($^\bullet$OH) in solutions can be used as an effective technology for the degradation of dye-containing wastewater.

- AOPs are confirmed as a highly competitive technology in water treatment for removing organic pollutants, especially dyes.
- Different types of AOPs, such as photocatalysis, photolysis, UV/H_2O_2, photolysis, UV/O_3, photo-Fenton, electrochemical oxidation, ozonation, sonolysis, etc., can be effectively used for the treatment of dye-containing wastewater.
- This paper thoroughly investigated the current utilization of photolysis and photocatalytic treatment processes, which are among effective AOPs, for the degradation of dye-containing wastewater.
- The study confirmed that photocatalysis could be used for the complete mineralization of various dyes present in water using light and a photocatalyst by the simultaneous occurrence of oxidation and reduction reactions.
- pH, the initial concentration of the dye, catalyst loading, etc., were identified to have an influence on the photocatalytic degradation of the dye.
- A recent development in the photocatalytic process using TiO_2 is the photocatalyst modification by metal and non-metal doping, which results in improved photocatalytic activity in the presence of visible radiation.
- Utilizing a cost-effective and sustainable energy source for the photocatalytic degradation of pollutants is very effective.
- Sunlight as energy for the photocatalytic degradation of various dyes and other organic pollutants will be more efficient in terms of energy utilization.
- The combination of various AOPs such as photocatalysis combined with sonolysis, ozonation, electrolysis, Fenton, etc., will be major aspects for the complete mineralization of various organic pollutants. It will be effective, as there is a synergistic effect, by combining one or more AOPs, which will eliminate the drawbacks of individual processes.
- Scaling up an energy-efficient, cost-effective, and sustainable technique for the complete mineralization of various types of organic pollutants from water by using a reusable energy source, sunlight, and individual AOPs or hybrid AOPs is the challenging future aspect.

References

1. Gürses, A.; Açıkyıldız, M.; Güneş, K.; Gürses, M.S. Dyes and pigments: Their structure and properties. In *Dyes and Pigments*; Springer: Berlin/Heidelberg, Germany, 2016; pp. 13–29.
2. Morsy, S.A.G.Z.; Tajudin, A.A.; Ali, M.S.M.; Shariff, F.M. Current development in decolorization of synthetic dyes by immobilized laccases. *Front. Microbiol.* **2020**, *11*, 572309. [CrossRef] [PubMed]
3. Benkhaya, S.M.; Rabet, S.; El Harfi, A. A review on classifications, recent synthesis and applications of textile dyes. *Inorg. Chem. Commun.* **2020**, *115*, 107891. [CrossRef]
4. Piaskowski, K.; Świderska-Dąbrowska, R.; anf Zarzycki, P.K. Dye removal from water and wastewater using various physical, chemical, and biological processes. *J. AOAC Int.* **2018**, *101*, 1371–1384. [CrossRef]
5. Chiu, Y.-H.; Chang, T.-F.; Chen, C.-Y.; Sone, M.; Hsu, Y.-J. Mechanistic insights into photodegradation of organic dyes using heterostructure photocatalysts. *Catalysts* **2019**, *9*, 430. [CrossRef]
6. Hunger, K. *Industrial Dyes: Chemistry, Properties, Applications*; Wiley-VCH Verlag GmbH & Co. KGaA: Weinheim, Germany, 2003.

7. Katheresan, V.; Kansedo, J.; Lau, S.Y. Efficiency of various recent wastewater dye removal methods: A review. *J. Environ. Chem. Eng.* **2018**, *6*, 4676–4697. [CrossRef]

8. Navarro, P.; Gabaldón, J.A.; Gómez-López, V.M. Degradation of an azo dye by a fast and innovative pulsed light/H_2O_2 advanced oxidation process. *Dye. Pigment.* **2017**, *136*, 887–892. [CrossRef]

9. Javaid, R.; Qazi, U.Y. Catalytic oxidation process for the degradation of synthetic dyes: An overview. *Int. J. Environ. Res. Public Health* **2019**, *16*, 2066. [CrossRef]

10. Carmen, Z.; Daniela, S. Textile organic dyes—Characteristics, polluting effects and separation/elimination procedures from industrial effluents-A critical overview. In *Organic Pollutants Ten Years after the Stockholm Convention—Environmental and Analytical Update*; IntechOpen: Rijeka, Croatia, 2012; pp. 55–86.

11. Ghaly, A.; Ananthashankar, R.; Alhattab, M.; Ramakrishnan, V. Production, characterization and treatment of textile effluents: A critical review. *J. Chem. Eng. Process Technol.* **2013**, *5*, 182.

12. Naveed, S.; Bhatti, I. Membrane technology and its suitability for treatment of textile wastewater in Pakistan. *J. Res.* **2006**, *17*, 155–164.

13. Mohajerani, M.; Mehrvar, M.; Ein-Mozaffari, F. An overview of the integration of advanced oxidation technologies and other processes for water and wastewater treatment. *Int. J. Eng. IJE* **2009**, *3*, 131.

14. Yagub, M.T.; Sen, T.K.; Afroze, S.; Ang, H.M. Dye and its removal from aqueous solution by adsorption: A review. *Adv. Colloid Interface Sci.* **2014**, *209*, 172–184. [CrossRef] [PubMed]

15. Adegoke, K.A.; Bello, O.S. Dye sequestration using agricultural wastes as adsorbents. *Water Resour. Ind.* **2015**, *12*, 8–24. [CrossRef]

16. Yeap, K.L.; Teng, T.T.; Poh, B.T.; Morad, N.; Lee, K.E. Preparation and characterization of coagulation/flocculation behavior of a novel inorganic–organic hybrid polymer for reactive and disperse dyes removal. *Chem. Eng. J.* **2014**, *243*, 305–314. [CrossRef]

17. Buthiyappan, A.; Abdul Aziz, A.R.; Wan Daud, W.M.A. Recent advances and prospects of catalytic advanced oxidation process in treating textile effluents. *Rev. Chem. Eng.* **2016**, *32*, 2. [CrossRef]

18. Muruganandham, M.; Suri, R.P.S.; Jafari, S.; Sillanpää, M.; Lee, G.-J.; Wu, J.J.; Swaminathan, M. Recent developments in homogeneous advanced oxidation processes for water and wastewater treatment. *Int. J. Photoenergy* **2014**, *2014*, 821674. [CrossRef]

19. Deng, Y.; Zhao, R. Advanced oxidation processes (AOPs) in wastewater treatment. *Curr. Pollut. Rep.* **2015**, *1*, 167–176. [CrossRef]

20. Peter, A.; Mihaly-Cozmuta, A.; Nicula, C.; Mihaly-Cozmuta, L.; Jastrzębska, A.; Olszyna, A.; Baia, L. UV light-assisted degradation of methyl orange, methylene blue, phenol, salicylic acid, and rhodamine B: Photolysis versus photocatalyis. *Water Air Soil Pollut.* **2017**, *228*, 1. [CrossRef]

21. Garrido-Cardenas, J.A.; Esteban-García, B.; Agüera, A.; Sánchez-Pérez, J.A.; Manzano-Agugliaro, F. Wastewater treatment by advanced oxidation process and their worldwide research trends. *Int. J. Environ. Res. Public Health* **2020**, *17*, 170. [CrossRef]

22. Khan, S.H.; Yadav, V.K. Advanced Oxidation Processes for Wastewater Remediation: An Overview. In *Removal of Emerging Contaminants Through Microbial Processes*; Springer: Singapore, 2021.

23. Britannica, T. (Ed.) Ultraviolet radiation. In *Encyclopedia Britannica*; 2021; Available online: https://www.britannica.com/science/ultraviolet-radiation (accessed on 15 June 2022).

24. Britannica, T. (Ed.) Heterogeneous reaction. In *Encyclopedia Britannica*; 1998; Available online: https://www.britannica.com/science/heterogeneous-reaction (accessed on 15 June 2022).

25. Britannica, T. (Ed.) Homogeneous reaction. In *Encyclopedia Britannica*; 2016; Available online: https://www.britannica.com/science/homogeneous-reaction (accessed on 15 June 2022).

26. Hossain, S.; Chun, D.-M. ZnO decorated polydimethylsiloxane sponges as photocatalysts for effective removal of methylene blue dye. *Mater. Chem. Phys.* **2020**, *255*, 123589. [CrossRef]

27. Mullapudi, V.B.K.; Salveru, A.; Kora, A.J. An in-house UV-photolysis setup for the rapid degradation of both cationic and anionic dyes in dynamic mode through UV/H_2O_2-based advanced oxidation process. *Int. J. Environ. Anal. Chem.* **2020**, *100*, 1–17. [CrossRef]

28. Lovato, M.E.; Fiasconaro, M.L.; Martín, C.A. Degradation and toxicity depletion of RB19 anthraquinone dye in water by ozone-based technologies. *Water Sci. Technol.* **2017**, *75*, 813–822. [CrossRef] [PubMed]

29. Fuentealba, D.; Venegas, C.; Morales, M.; Waissbluth, O. Comparing photo-Fenton degradation of malachite green using FeII and FeIII salts under UVA light irradiation. *J. Braz. Chem. Soc.* **2016**, *27*, 341–348.

30. Chanikya, P.; Nidheesh, P.V.; Babu, D.S.; Gopinath, A.; Kumar, M.S. Treatment of dyeing wastewater by combined sulfate radical based electrochemical advanced oxidation and electrocoagulation processes. *Sep. Purif. Technol.* **2021**, *254*, 117570. [CrossRef]

31. Dias, N.C.; Bassin, J.P.; Sant'Anna, G.L.; Dezotti, M. Ozonation of the dye reactive red 239 and biodegradation of ozonation products in a moving-bed biofilm reactor: Revealing reaction products and degradation pathways. *Int. Biodeterior. Biodegrad.* **2019**, *144*, 104742. [CrossRef]

32. Eren, Z.; Ince, N.H. Sonolytic and sonocatalytic degradation of azo dyes by low and high frequency ultrasound. *J. Hazard. Mater.* **2010**, *177*, 1019–1024. [CrossRef]

33. Vilhunen, S.; Sillanpää, M. Recent developments in photochemical and chemical AOPs in water treatment: A mini-review. *Rev. Environ. Sci. Bio/Technol.* **2010**, *9*, 323–330. [CrossRef]

34. Khan, I.; Saeed, K.; Ali, N.; Khan, I.; Zhang, B.; Sadiq, M. Heterogeneous photodegradation of industrial dyes: An insight to different mechanisms and rate affecting parameters. *J. Environ. Chem. Eng.* **2020**, *8*, 104364. [CrossRef]

35. Rafiq, A.; Ikram, M.; Ali, S.; Niaz, F.; Khan, M.; Khan, Q.; Maqbool, M. Photocatalytic degradation of dyes using semiconductor photocatalysts to clean industrial water pollution. *J. Ind. Eng. Chem.* **2021**, *97*, 111–112. [CrossRef]

36. Hashimoto, K.; Irie, H.; Fujishima, A. TiO$_2$ photocatalysis: A historical overview and future prospects. *Jpn. J. Appl. Phys.* **2005**, *44*, 8269–8285. [CrossRef]

37. Gallagher, R.P.; Lee, T.K.; Bajdik, C.D.; Borugian, M. Ultraviolet radiation. *Chronic Dis. Inj. Can.* **2010**, *29*, 51–68. [CrossRef]

38. Cuerda-Correa, E.M.; Alexandre-Franco, M.F.; Fernández-González, C. Advanced oxidation processes for the removal of antibiotics from water. An overview. *Water* **2019**, *12*, 102. [CrossRef]

39. Mohammed, H.A.; Khaleefa, S.A.; Basheer, I.M. Photolysis of methylene blue dye using an advanced oxidation process (ultraviolet light and hydrogen peroxide). *J. Eng. Sustain. Dev.* **2021**, *25*, 59–67. [CrossRef]

40. Asano, T.; Burton, F.; Leverenz, H. Water reuse. In *Issues, Technologies and Applications*, 1st ed.; Inc. Metcalf and Eddy, McGraw-Hill Companies Inc.: New York, NY, USA, 2006.

41. Navarro, P.; Zapata, J.P.; Gotor, G.; Gonzalez-Olmos, R.; Gómez-López, V.M. Degradation of malachite green by a pulsed light/H$_2$O$_2$ process. *Water Sci. Technol.* **2019**, *79*, 260–269. [CrossRef]

42. Joseph, C.; Taufiq-Yap, Y.H.; Elilarasi, L.; Krishnan, V. Remediation of cationic dye simulated wastewater using photolysis: Parametric and kinetic studies. *Malays. J. Chem.* **2017**, *19*, 82–98.

43. Jamal, M.; Muneer, M.; Iqbal, M. Photo-degradation of monoazo dye blue 13 using advanced oxidation process. *Chem. Int.* **2015**, *1*, 12–16.

44. De Lima, L.B.; Pereira, L.O.; de Moura, S.G.; Magalhães, F. Degradation of organic contaminants in effluents—Synthetic and from the textile industry-by Fenton, photocatalysis, and H$_2$O$_2$ photolysis. *Environ. Sci. Pollut. Res.* **2016**, *24*, 6299–6306. [CrossRef]

45. Grčić, I.; Papić, S.; Mesec, D.; Koprivanac, N.; Vujević, D. The kinetics and efficiency of UV assisted advanced oxidation of various types of commercial organic dyes in water. *J. Photochem. Photobiol. A Chem.* **2014**, *273*, 49–58. [CrossRef]

46. Nikravesh, B.; Shomalnasab, A.; Nayyer, A.; Aghababaei, N.; Zarebi, R.; Ghanbari, F. UV/Chlorine process for dye degradation in aqueous solution: Mechanism, affecting factors and toxicity evaluation for textile wastewater. *J. Environ. Chem. Eng.* **2020**, *8*, 104244. [CrossRef]

47. Wang, S.; Luo, C.; Tan, F.; Cheng, X.; Ma, Q.; Wu, D.; Li, P.; Zhang, F.; Ma, J. Degradation of Congo red by UV photolysis of nitrate: Kinetics and degradation mechanism. *Sep. Purif. Technol.* **2021**, *262*, 118276. [CrossRef]

48. Wen, D.; Li, W.; Lv, J.; Qiang, Z.; Li, M. Methylene blue degradation by the VUV/UV/persulfate process: Effect of pH on the roles of photolysis and oxidation. *J. Hazard. Mater.* **2020**, *391*, 121855. [CrossRef]

49. Bendjama, H.; Merouani, S.; Hamdaoui, O.; Bouhelassa, M. UV-photolysis of Chlorazol Black in aqueous media: Process intensification using acetone and evidence of methyl radical implication in the degradation process. *J. Photochem. Photobiol. A Chem.* **2019**, *368*, 268–275. [CrossRef]

50. Ghodbane, H.; Hamdaoui, O. Decolorization of antraquinonic dye, C.I. Acid Blue 25, in aqueous solution by direct UV irradiation, UV/ H$_2$O$_2$ and UV/Fe(II) processes. *Chem. Eng. J.* **2010**, *160*, 226–231. [CrossRef]

51. Egerton, T.A.; Purnama, H. Does hydrogen peroxide really accelerate TiO$_2$ UV-C photocatalyzed decolouration of azo-dyes such as reactive orange 16? *Dye. Pigment.* **2014**, *101*, 280–285. [CrossRef]

52. Mitrovic, J.; Radovic, M.; Bojic, D.; Andjelkovic, T.; Purenovic, M.; Bojic, A. Decolorization of textile azo dye reactive orange 16 with UV/ H$_2$O$_2$ process. *J. Serb. Chem. Soc.* **2012**, *77*, 465–481. [CrossRef]

53. Guimarães, J.R.; Guedes Maniero, M.; de Araújo, R.N. A comparative study on the degradation of RB-19 dye in an aqueous medium by advanced oxidation processes. *J. Environ. Manag.* **2012**, *110*, 33–39. [CrossRef] [PubMed]

54. Ma, C.-M.; Hong, G.-B.; Chen, H.-W.; Hang, N.-T.; Shen, Y.-S. Photooxidation contribution study on the decomposition of azo dyes in aqueous solutions by VUV-based AOPs. *Int. J. Photoenergy* **2011**, *2011*, 156456. [CrossRef]

55. Dhruv, B.; Abhipsa, M. UV/Fe^{+3} Photolysis process optimization using response surface methodology for decolorization of reactive red 120 dye simulated wastewater. In *Recent Trends in Civil Engineering*; Springer: Singapore, 2021.

56. Zuorro, A.; Lavecchia, R. Evaluation of UV/ H$_2$O$_2$ advanced oxidation process (AOP) for the degradation of diazo dye reactive green 19 in aqueous solution. *Desalination Water Treat.* **2014**, *52*, 1571–1577. [CrossRef]

57. Marhoon, A.A.; Saeed, S.I.; Ahmed, L.M. Application of some effects on the degradation of the aqueous solution of fuchsine dye by photolysis. *J. Glob. Pharma Technol.* **2019**, *11*, 76–81.

58. Gole, V.L.; Gogate, P.R. Degradation of brilliant green dye using combined treatment strategies based on different irradiations. *Sep. Purif. Technol.* **2014**, *133*, 212–220. [CrossRef]

59. Sartaj, S.; Ali, N.; Khan, A.; Malik, S.; Bilal, M.; Khan, M.; Ali, N.; Hussain, S.; Khan, H.; Khan, S. Performance evaluation of photolytic and electrochemical oxidation processes for enhanced degradation of food dyes laden wastewater. *Water Sci. Technol.* **2020**, *81*, 971–984. [CrossRef]

60. Kalsoom, U.; Ashraf, S.S.; Meetani, M.A.; Rauf, M.A.; Bhatti, H.N. Degradation and kinetics of H$_2$O$_2$ assisted photochemical oxidation of Remazol Turquoise Blue. *Chem. Eng. J.* **2012**, *200*, 373–379. [CrossRef]

61. Rauf, M.A.; Marzouki, N.; Körbahti, B.K. Photolytic decolorization of Rose Bengal by UV/H$_2$O$_2$ and data optimization using response surface method. *J. Hazard. Mater.* **2008**, *159*, 602–609. [CrossRef] [PubMed]

62. Aliouche, S.; Djebbar, K.; Sehili, T. Removal of an azo dye (Alizarin yellow) in homogeneous medium using direct photolysis, acetone/UV, H$_2$O$_2$/UV, /UV, H$_2$O$_2$//UV, and /heat. *Desalination Water Treat.* **2016**, *57*, 18182–18193. [CrossRef]

63. Körbahti, B.K.; Rauf, M.A. Determination of optimum operating conditions of carmine decoloration by UV/H$_2$O$_2$ using response surface methodology. *J. Hazard. Mater.* **2009**, *161*, 281–286. [CrossRef] [PubMed]

64. Elmorsi, T.M.; Riyad, Y.M.; Mohamed, Z.H.; Abd El Bary, H.M.H. Decolorization of mordant red 73 azo dye in water using H$_2$O$_2$/UV and photo-Fenton treatment. *J. Hazard. Mater.* **2010**, *174*, 352–358. [CrossRef]

65. Bousnoubra, I.; Djebbar, K.; Abdessemed, A.; Sehili, T. Decolorization of methyl green and bromocresol purple in mono and binary systems by photochemical processes: Direct UV photolysis, Acetone/UV and H$_2$O$_2$/UV. A comparative study. *Desalination Water Treat.* **2016**, *57*, 27710–27725. [CrossRef]

66. Chenini, H.; Djebbar, K.; Zendaoui, S.M.; Sehili, T.; Zouchoune, B. Removal of an azo dye (Orange G) by various methods in homogeneous phase: Comparative study. *Jordan J. Chem.* **2011**, *6*, 307–319.

67. Ding, X.; Gutierrez, L.; Croue, J.-P.; Li, M.; Wang, L.; Wang, Y. Hydroxyl and sulfate radical-based oxidation of RhB dye in UV/H$_2$O$_2$ and UV/persulfate systems: Kinetics, mechanisms, and comparison. *Chemosphere* **2020**, *253*, 126655. [CrossRef]

68. Maleki, A.; Mahvi, A.H.; Ebrahimi, R.; Zandsalimi, Y. Study of photochemical and sonochemical processes efficiency for degradation of dyes in aqueous solution. *Korean J. Chem. Eng.* **2010**, *27*, 1805–1810. [CrossRef]

69. Kasiri, M.B.; Khataee, A.R. Photooxidative decolorization of two organic dyes with different chemical structures by UV/H$_2$O$_2$ process: Experimental design. *Desalination* **2011**, *270*, 151–159. [CrossRef]

70. Haji, S.; Benstaali, B.; Al-Bastaki, N. Degradation of methyl orange by UV/H$_2$O$_2$ advanced oxidation process. *Chem. Eng. J.* **2011**, *168*, 134–139. [CrossRef]

71. Jian-xiao, L.V.; Ying, C.; Guo-hong, X.; Ling-yun, Z.; Su-fen, W. Decoloration of methylene blue simulated wastewater using a UV-H$_2$O$_2$ combined system. *J. Water Reuse Desalination* **2011**, *1*, 45–51. [CrossRef]

72. Chekir, N.; Tassalit, D.; Benhabiles, O.; Kasbadji Merzouk, N.; Ghenna, M.; Abdessemed, A.; Issaadi, R. A comparative study of tartrazine degradation using UV and solar fixed bed reactors. *Int. J. Hydrogen Energy* **2017**, *42*, 8948–8954. [CrossRef]

73. Zukawa, T.; Sasaki, Y.; Kurosawa, T.; Kamiko, N. Photolysis of Indigo Carmine solution by planar vacuum-ultraviolet (147 nm) light source. *Chemosphere* **2019**, *214*, 123–129. [CrossRef]

74. Safni, M.; Putri, R.; Wellia, D.; Septiani, U. Photodegradation of orange F3R dyes: Effect of light sources and the addition of CN—Codoped TiO$_2$ catalyst. *Pharma Chem.* **2017**, *9*, 1–5.

75. Algubili, A.M.; Alrobayi, E.M.; Alkaim, A.F. Photocatalytic degradation of remazol brilliant blue dye by ZnO/UV process. *Int. J. Chem. Sci.* **2015**, *13*, 911–921.

76. Daneshvar, N.; Behnajady, M.A.; Mohammadi, M.K.A.; Dorraji, M.S.S. UV/H$_2$O$_2$ treatment of rhodamine b in aqueous solution: Influence of operational parameters and kinetic modeling. *Desalination* **2008**, *230*, 16–26. [CrossRef]

77. Soltani, T.; Entezari, M.H. Photolysis and photocatalysis of methylene blue by ferrite bismuth nanoparticles under sunlight irradiation. *J. Mol. Catal. A Chem.* **2013**, *377*, 197–203. [CrossRef]

78. Mishra, N.; Reddy, R.; Kuila, A.; Rani, A.; Nawaz, A.; Pichiah, S. A review on advanced oxidation processes for effective water treatment. *Curr. World Environ.* **2017**, *12*, 469–489. [CrossRef]

79. Damodar, R.A.; You, S.-J. Performance of an integrated membrane photocatalytic reactor for the removal of Reactive Black 5. *Sep. Purif. Technol.* **2010**, *71*, 44–49. [CrossRef]

80. Bansal, P.; Sud, D. Photodegradation of commercial dye, Procion Blue HERD from real textile wastewater using nanocatalysts. *Desalination* **2011**, *267*, 244–249. [CrossRef]

81. Soni, H.; Kumar, N.J.I. UV light induced photocatalytic degradation of malachite green on TiO$_2$ nanoparticles. *Int. J. Recent Res. Rev.* **2014**, *3*, 10–15.

82. Putri, R.A.; Safni, S.; Jamarun, N.; Septiani, U.; Kim, M.-K.; Zoh, K.-D. Degradation and mineralization of violet-3B dye using C-N-codoped TiO$_2$ photocatalyst. *Environ. Eng. Res.* **2020**, *25*, 529–535. [CrossRef]

83. Gupta, V.K.; Jain, R.; Nayak, A.; Agarwal, S.; Shrivastava, M. Removal of the hazardous dye—Tartrazine by photodegradation on titanium dioxide surface. *Mater. Sci. Eng. C* **2011**, *31*, 1062–1067. [CrossRef]

84. Hadjltaief, B.H.; Ben Zina, M.; Galvez, M.E.; Da Costa, P. Photocatalytic degradation of methyl green dye in aqueous solution over natural clay-supported ZnO–TiO$_2$ catalysts. *J. Photochem. Photobiol. A Chem.* **2016**, *315*, 25–33. [CrossRef]

85. Lee, P.-W.; Ong, S.-T.; Hung, Y.-T.; Lee, S.-L. Photodegradation of malachite green by immobilization of titanium dioxide on glass plates. *Asian J. Chem.* **2013**, *25*, 755–758. [CrossRef]

86. Bindhu, M.R.; Willington, T.D.; Hatshan, M.R.; Chen, S.-M.; Chen, T.-W. Environmental photochemistry with Sn/F simultaneously doped TiO$_2$ nanoparticles: UV and visible light induced degradation of thiazine dye. *Environ. Res.* **2022**, *207*, 112108. [CrossRef]

87. Sharma, S.K.; Bhunia, H.; Bajpai, P.K. Photocatalytic decolorization kinetics and mineralization of Reactive Black 5 aqueous solution by UV/TiO$_2$ nanoparticles. *CLEAN—Soil Air Water* **2012**, *40*, 1290–1296. [CrossRef]

88. Jawad, A.H.; Mubarak, N.S.A.; Ishak, M.A.M.; Ismail, K.; Nawawi, W.I. Kinetics of photocatalytic decolourization of cationic dye using porous TiO$_2$ film. *J. Taibah Univ. Sci.* **2018**, *10*, 352–362. [CrossRef]

89. Joseph, C.G.; Taufiq-Yap, Y.H.; Puma, G.L.; Sanmugam, K.; Quek, K.S. Photocatalytic degradation of cationic dye simulated wastewater using four radiation sources, UVA, UVB, UVC and solar lamp of identical power output. *Desalination Water Treat.* **2016**, *57*, 7976–7987. [CrossRef]

90. Laohaprapanon, S.; Matahum, J.; Tayo, L.; You, S.-J. Photodegradation of Reactive Black 5 in a ZnO/UV slurry membrane reactor. *J. Taiwan Inst. Chem. Eng.* **2015**, *49*, 136–141. [CrossRef]

91. Kansal, S.K.; Kaur, N.; Singh, S. Photocatalytic degradation of two commercial reactive dyes in aqueous phase using nanophoto-catalysts. *Nanoscale Res. Lett.* **2009**, *4*, 709–716. [CrossRef] [PubMed]

92. Kong, J.-Z.; Li, A.-D.; Li, X.-Y.; Zhai, H.-F.; Zhang, W.-Q.; Gong, Y.-P.; Li, H.; Wu, D. Photo-degradation of methylene blue using Ta-doped ZnO nanoparticle. *J. Solid State Chem.* **2010**, *183*, 1359–1364. [CrossRef]

93. Juang, R.-S.; Lin, S.-H.; Hsueh, P.-Y. Removal of binary azo dyes from water by UV-irradiated degradation in TiO_2 suspensions. *J. Hazard. Mater.* **2010**, *182*, 820–826. [CrossRef]

94. Vaiano, V.; Sacco, O.; Sannino, D.; Ciambelli, P. Nanostructured N-doped TiO_2 coated on glass spheres for the photocatalytic removal of organic dyes under UV or visible light irradiation. *Appl. Catal. B Environ.* **2015**, *170*, 153–161. [CrossRef]

95. Shinde, D.R.; Tambade, P.S.; Chaskar, M.G.; Gadave, K.M. Photocatalytic degradation of dyes in water by analytical reagent grades ZnO, TiO_2 and SnO_2: A comparative study. *Drink. Water Eng. Sci.* **2017**, *10*, 109–117. [CrossRef]

96. Tolia, J.; Chakraborty, M.; Murthy, Z. Photocatalytic degradation of malachite green dye using doped and undoped ZnS nanoparticles. *Pol. J. Chem. Technol.* **2012**, *14*, 16–21. [CrossRef]

97. Azami, M.S.; Nawawi, W.I.; Jawad, A.H.; Ishak, M.A.M.; Ismail, K. N-doped TiO_2 synthesised via microwave induced photocat-alytic on RR4 dye removal under LED light irradiation. *Sains Malays.* **2017**, *46*, 1309–1316. [CrossRef]

98. Tammina, S.K.; Mandal, B.K.; Kadiyala, N.K. Photocatalytic degradation of methylene blue dye by nonconventional synthesized SnO_2 nanoparticles. *Environ. Nanotechnol. Monit. Manag.* **2018**, *10*, 339–350. [CrossRef]

99. Khatri, A.; Rana, P.S. Visible light assisted photocatalysis of Methylene Blue and Rose Bengal dyes by iron doped NiO nanoparticles prepared via chemical co-precipitation. *Phys. B Condens. Matter* **2020**, *579*, 411905. [CrossRef]

100. Reddy, C.V.; Reddy, I.N.; Ravindranadh, K.; Reddy, K.R.; Kim, D.; Shim, J. Ni-dopant concentration effect of ZrO_2 photocatalyst on photoelectrochemical water splitting and efficient removal of toxic organic pollutants. *Sep. Purif. Technol.* **2020**, *252*, 117352. [CrossRef]

101. Nguyen, C.H.; Fu, C.-C.; Juang, R.-S. Degradation of methylene blue and methyl orange by palladium-doped TiO2 photocatalysis for water reuse: Efficiency and degradation pathways. *J. Clean. Prod.* **2018**, *202*, 413–427. [CrossRef]

102. Tichapondwa, S.M.; Newman, J.P.; Kubheka, O. Effect of TiO_2 phase on the photocatalytic degradation of methylene blue dye. *Phys. Chem. Earth Parts A/B/C* **2020**, *118*, 102900. [CrossRef]

103. Kazeminezhad, I.; Sadollahkhani, A. Influence of pH on the photocatalytic activity of ZnO nanoparticles. *J. Mater. Sci. Mater. Electron.* **2016**, *27*, 4206–4215. [CrossRef]

104. Azzaz, A.A.; Assadi, A.A.; Jellali, S.; Bouzaza, A.; Wolbert, D.; Rtimi, S. Discoloration of simulated textile effluent in contin-uous photoreactor using immobilized titanium dioxide: Effect of zinc and sodium chloride. *J. Photochem. Photobiol. A Chem.* **2018**, *358*, 111–120. [CrossRef]

105. Anwer, H.; Mahmood, A.; Lee, J.; Kim, K.-H.; Park, J.-W.; Yip, A.C.K. Photocatalysts for degradation of dyes in industrial effluents: Opportunities and challenges. *Nano Res.* **2019**, *12*, 955–972. [CrossRef]

106. Sacco, O.; Stoller, M.; Vaiano, V.; Ciambelli, P.; Chianese, A.; Sannino, D. Photocatalytic degradation of organic dyes under visible light on N-doped TiO_2 Photocatalysts. *Int. J. Photoenergy* **2012**, *2012*, 626759. [CrossRef]

107. Khan, T.T.; Bari, G.A.K.M.R.; Kang, H.-J.; Lee, T.-G.; Park, J.-W.; Hwang, H.; Hossain, S.; Mun, J.; Suzuki, N.; Fujishima, A.; et al. Synthesis of N-doped TiO_2 for efficient photocatalytic degradation of atmospheric NOx. *Catalysts* **2021**, *11*, 109. [CrossRef]

108. Al-Mamun, M.R.; Kader, S.; Islam, M.S.; Khan, M.Z.H. Photocatalytic activity improvement and application of UV-TiO2 photocatalysis in textile wastewater treatment: A review. *J. Environ. Chem. Eng.* **2019**, *7*, 103248. [CrossRef]

109. Wu, Y.; Xing, M.; Zhang, J. Gel-hydrothermal synthesis of carbon and boron co-doped TiO_2 and evaluating its photocatalytic activity. *J. Hazard. Mater.* **2011**, *192*, 368–373. [CrossRef]

110. Eskandarian, M.R.; Ganjkhanloo, M.; Rasoulifard, M.H.; Hosseini, S.A. Energy-efficient removal of acid red 14 by UV-LED/persulfate advanced oxidation process: Pulsed irradiation, duty cycle, reaction kinetics, and energy consumption. *J. Taiwan Inst. Chem. Eng.* **2021**, *127*, 129–139. [CrossRef]

111. Bolton, J.R.; Bircher, K.G.; Tumas, W.; Tolman, C.A. Figures-of-merit for the technical development and application of advanced oxidation technologies for both electric- and solar-driven systems (IUPAC Technical Report). *Pure Appl. Chem.* **2001**, *73*, 627–637. [CrossRef]

112. Raju, A.; Vishnuganth, M.; Asha, R.; Remya, N.; Selvaraju, N.; Kumar, M. Livestock wastewater treatment in batch and continuous photocatalytic systems: Performance and economic analyses. *Water Air Soil Pollut.* **2015**, *226*, 132.

113. Basturk, E.; Karatas, M. Decolorization of antraquinone dye Reactive Blue 181 solution by UV/H_2O_2 process. *J. Photochem. Photobiol. A Chem.* **2015**, *299*, 67–72. [CrossRef]

114. Rabahi, A.; Assadi, A.A.; Nasrallah, N. Photocatalytic treatment of petroleum industry wastewater using recirculating annular reactor: Comparison of experimental and modeling. *Environ. Sci. Pollut. Res.* **2019**, *26*, 19035–19046. [CrossRef]